

1 **Title.** Physicochemical Factors and Urban Land-Use Characteristics Associated with Resistance
2 to Precipitation in Estuaries Vary Across Scales

3

4 **Authors and Affiliations**

5 *Anna B. Turetcaia 0000-0003-1630-5741¹, anna.turetcaia@pnnl.gov*

6 *Nicole G. Dix 0000-0002-0063-5167², nikki.dix@dep.state.fl.us*

7 *Hannah Ramage 0009-0004-2246-7696³, hannah.ramage@wisc.edu*

8 *Matthew C. Ferner 0000-0002-4862-9663⁴, mferner@sfsu.edu*

9 *Emily B. Graham 0000-0002-4623-7076^{1,5}, emily.graham@pnnl.gov*

10

11 ¹ Pacific Northwest National Laboratory, Richland, WA 99352, USA

12 ² Guana Tolomato Matanzas National Estuarine Research Reserve, Ponte Vedra Beach, FL
13 32082, USA

14 ³ Lake Superior National Estuarine Research Reserve, University of Wisconsin Madison,
15 Division of Extension, Superior, WI 54880, USA

16 ⁴ San Francisco State University, Estuary and Ocean Science Center, Tiburon, CA 94920, USA

17 ⁵ School of Biological Sciences, Washington State University, Pullman, WA 99164, USA

18

19 **Corresponding authors:** *Anna B. Turetcaia (anna.turetcaia@pnnl.gov) and Emily B. Graham*
20 *(emily.graham@pnnl.gov)*

21 ***Abstract***

22 Urban estuaries are subject to frequent stressors, including nutrient loading and
23 hydrological flashiness, which worsen water quality and disrupt ecosystem function. Land use
24 changes associated with urbanization, as well as atypical precipitation conditions can exacerbate
25 stress on estuarine health. However, generalizable patterns and parameters involved in estuarine
26 responses to urbanization and extreme precipitation events remain unknown. We investigated
27 physicochemical factors and urban land-use characteristics that associate with estuarine
28 resistance to precipitation within and across estuaries ranging in urbanization, salinity, and
29 precipitation. Using population and land use/land cover data combined with long-term
30 meteorological, nutrient, and water quality data from the National Estuarine Research Reserve
31 System, we focused on five estuaries distributed across the continental United States. We
32 hypothesized that estuaries with higher urban impact exhibit lower resistance to precipitation
33 events. We investigate this through relationships between the resistance index – a proxy for
34 ecosystem stability calculated using dissolved oxygen – and various physicochemical factors and
35 urban land-use characteristics on local and continental scales. Contrary to our hypothesis, we
36 found that estuaries with higher urban influences were more resistant to precipitation events, and
37 that water temperature, water column depth, nitrogen, and chlorophyll-*a* were related to estuarine
38 resistance on a continental scale. However, these trends interacted with estuarine salinity and
39 varied across individual estuaries; where we found additional relationships of resistance with
40 salinity, turbidity, phosphate concentrations, N:P ratio, and tree cover. Considering emerging
41 stressors from new climatic scenarios and urbanization-driven changes, these results are
42 important for informing decisions for determining the appropriate estuarine water-quality
43 standards.

44

45 ***Introduction***

46 Estuaries are highly dynamic environments that often connect freshwater and saltwater
47 systems, cycle organic matter and nutrients from land to oceans, and provide essential ecosystem
48 services (Bianchi, 2007; He & Silliman, 2019). Estuarine ecosystem function, which relies on
49 stability of a predictable range of dynamic processes like temperature fluctuations, hydrology
50 and nutrient mixing, is threatened by anthropogenic activities and extreme climatic events like
51 storms (Kemp et al., 2009; Zhang et al., 2010). Yet, generalizable factors involved in resistance
52 of ecosystem function to precipitation in freshwater and saltwater estuaries impacted by
53 urbanization are not fully understood. Predicted increases in urban population size and in
54 frequency and intensity of precipitation events (Kyzar et al., 2021; Li et al., 2019; Martínez et al.,
55 2007; Pickett et al., 2011) highlight the urgency to understand the response of estuaries to new
56 urban and climatic scenarios.

57 When combined with intense precipitation, watershed urbanization and associated
58 changes in land use/land cover (LULC) (Grimm et al., 2008) often result in increases in stream
59 hydrological flashiness (Gannon et al., 2022; Reisinger et al., 2017). Triggered by extreme
60 precipitation, hydrological flashing induces increased flow rates that cause changes in channel
61 morphology (Booth & Jackson, 1997; Gregory, 2011; Leopold, 1968; Vietz et al., 2016), habitat
62 destruction (Walsh et al., 2005), and disruption of microbial metabolic processes (Reisinger et
63 al., 2017; Uehlinger, 2000). Flashiness can also drastically affect in-stream primary production
64 (e.g., phytoplankton) – a critical component of dissolved oxygen (DO) delivery to aquatic
65 environments – through increases in flow velocity, transport of phytoplankton, and light
66 limitation (Bernot et al., 2010; Fisher et al., 1982; Reisinger et al., 2017; Uehlinger, 2000).

67 Additionally, extreme precipitation events are often associated with excess nitrogen (N)
68 delivery, particularly for streams adjacent to urban-type LULC (Walsh et al., 2005). Nitrogen is
69 central to mediating ecosystem functions across systems and urbanization gradients (Mulholland
70 et al., 2008; Schindler, 1977; S. V. Smith, 1984; Vitousek & Howarth, 1991). It is particularly
71 important for primary production because many phytoplankton species are N-limited (Evans &
72 Seemann, 1989; Howarth, 1988; Vitousek & Howarth, 1991). This means that N directly affects
73 DO production in aquatic environments. Therefore, N delivery associated with precipitation
74 could temporarily have a positive effect on phytoplankton community rebound, DO

75 concentrations, and functional stability in estuaries impacted by urbanization. Also, extreme
76 precipitation events are often associated with influx of freshwater and/or saltwater into estuaries,
77 which changes salinity and impacts ecosystem metabolic functions. However, depending on the
78 temporal and spatial scales of evaluation, the reported trends of system responses to precipitation
79 and salinity changes can be conflicting.

80 Trends for stream responses to disturbances identified on continental-scale (i.e.,
81 regardless of system specifics) can help in projecting long-term ecosystem function under
82 changing climatic and urban conditions, but they have been difficult to decipher due to variation
83 across local scales. While Ombadi & Varadharajan (2022) report contrasting effects of
84 urbanization on salinity during flood events when regional climatic conditions were considered,
85 a continental-scale study by Kaushal et al. (2018) suggests that anthropogenic activity is
86 associated with increasing salinity in streams over time. However, the later study recognizes that
87 regional, climatic, LULC, and geologic variabilities also influence stream salinization patterns.
88 Similarly, continental-scale evaluations showed that streams within small watersheds appear
89 consistently less flashy than streams in large watersheds; while there was a substantial amount of
90 variability in these relationships at regional scale (Baker et al., 2004; Gannon et al., 2022;
91 Hopkins et al., 2015; Poff et al., 2006). Such variation in relationships across scales may be
92 particularly prevalent in ecosystems influenced by anthropogenic activities (Hopkins et al., 2015;
93 Poff et al., 2006). This demonstrates the importance of considering multiple spatial scales in
94 understanding ecosystem responses to changes in precipitation patterns and watershed land use.

95 We aim to uncover generalizable patterns of responses to precipitation events across
96 estuaries in the continental U.S. across gradients of urbanization and physicochemical properties.
97 Using DO as a response variable and a proxy for ecosystem function, we evaluate estuary
98 resistance to precipitation in the context of physicochemical factors and land-use characteristics
99 at: 1) the continental-scale (i.e., across all estuaries); 2) across estuaries grouped by average
100 annual salinity; and 3) within each estuary. We hypothesize that urbanization decreases estuarine
101 resistance to precipitation. Also, we expect that relationships between resistance and
102 physicochemical factors and land-use characteristics will diverge with spatial scale. Moreover,
103 we expect that salinity impacts estuarine resistance to precipitation because of its effects on DO
104 solubility and phytoplankton biomass. This study is essential for understanding how ongoing
105 changes in climate and urbanization conditions influence estuarine ecosystem health.

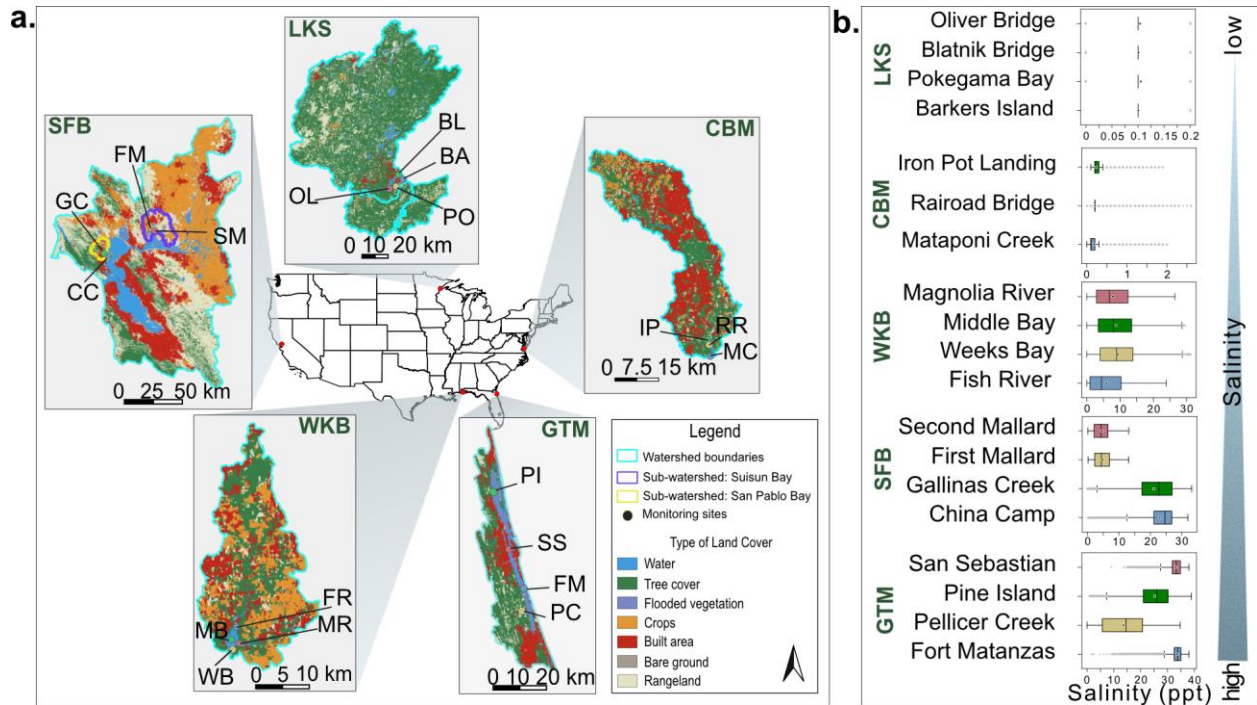
106

107 **Methods**

108 **Study sites.**

109 We used long-term water quality monitoring data from five estuaries in the National
110 Estuarine Research Reserve System (NERRS, <https://coast.noaa.gov/nerrs/>) to understand factors
111 associated with ecosystem resistance to precipitation events. Lake Superior (LKS), WI;
112 Chesapeake Bay Maryland (CBM), MD (Jug Bay only); Guana Tolomato Matanzas (GTM), FL;
113 Weeks Bay (WKB), AL; and San Francisco Bay (SFB), CA span climatic zones, land uses, and
114 salinity (range: 0.1 - 35 ppt) (Fig. 1, Table 1). Across all estuaries, there were a total of 19
115 monitoring locations (3 at CBM, and 4 at LKS, GTM, WKB, and SFB). Dissolved oxygen, water
116 temperature, conductivity, pH, turbidity, salinity, water column depth, and meteorological
117 conditions are measured at 15-min intervals. PO_4^{3-} , NO_3^- , NH_4^+ , NO_2^- and chlorophyll-*a* (Chl-*a*)
118 were measured monthly (NERRS, 2023). Water column depth was calculated as the sum of
119 measured water depth and depth of the monitoring probe to the sediment bed. The sum of NO_3^- ,
120 NO_2^- , and NH_4^+ was used to assess dissolved inorganic nitrogen (DIN) concentrations, and DIN
121 to PO_4^{3-} was used to calculate N:P mass ratio. Also, we used data from two years at each estuary
122 between 2016 to 2020; one relatively wet year and one relatively dry year to span different
123 baseline hydrologic and chemical conditions (see below). We removed all data flagged as
124 ‘suspect’ or ‘out of range’.

125



126

127 **Fig. 1.** Selected National Estuarine Research Reserve (NERR) stations. a) Map of monitoring
 128 locations and land use/land cover within associated watersheds at Lake Superior (LKS) NERR,
 129 Chesapeake Bay, Maryland (CBM) NERR, Guana Tolomato Matanzas (GTM) NERR, Weeks
 130 Bay (WKB) NERR, and San Francisco Bay (SFB) NERR. b) Salinity from 2012 to 2022 for each
 131 monitoring location at each NERR (all $n > 150,000$). Boxes indicate interquartile range. Means
 132 are shown in black-and-white circles. Black lines indicate medians.

133

134 **Watershed characteristics.**

135 To assess the relationships between resistance and urbanization, we used NERR
 136 watershed boundaries from <https://cdmo.baruch.sc.edu> (NERRS, 2023), LULC data at 10-meter
 137 resolution from Esri (<https://livingatlas.arcgis.com/landcover/>), and U.S. (2020) constrained
 138 population density data at 100-meter resolution from World Population Hub
 139 (<https://www.worldpop.org/>) (Bondarenko et al., 2020). We used LULC data from 2020 (LKS),
 140 2018 (CBM, SFB), and 2017 (GTM, WKB) to keep the LULC within the range of wet and dry
 141 years selected for each estuary (see below). Analyses of LULC and population density were
 142 performed in QGIS 3.30.3 (QGIS Development Team, 2023) equipped with a semi-automatic
 143 classification plug-in.

144 Further, because the resistance index was calculated for precipitation events across short
 145 time-scales (i.e., days), which underrepresents the draining time of some watersheds, we
 146 considered LULC and population density from a 10-km proximity zone to the monitoring
 147 locations (Table 1). For SFB NERR, we used 10-km proximity zones from San Pablo and Suisun
 148 embayments to quantify LULC and population density, because the embayments separate China
 149 Camp and Gallinas Creek from First Mallard and Second Mallard monitoring locations,
 150 respectively.

151

152 **Table 1:** Land use/land cover (LULC) and population density in each estuary.

LULC class	Estuary and % area by LULC class					
	Top number: watershed scale					
	<i>Bottom number:</i> local scale (within 10 km of the monitoring locations)					
	<i>LKS</i>	<i>CBM</i> <i>(Jug Bay)</i>	<i>GTM</i>	<i>WKB</i>	<i>SFB</i>	
					<i>(San Pablo Bay) CC, GC</i>	<i>(Suisun Bay) FM, SM</i>
Water	3.62 <i>10.43</i>	0.97 <i>2.30</i>	6.78 <i>8.58</i>	2.19 <i>4.85</i>	5.02 <i>5.04</i>	2.32 <i>3.59</i>
Tree cover	73.1 <i>58.78</i>	38.34 <i>53.72</i>	45.67 <i>45.11</i>	39.58 <i>38.52</i>	26.47 <i>26.91</i>	0.8 <i>1.16</i>
Flooded vegetation	0.2 <i>0.88</i>	0.22 <i>1.37</i>	9.48 <i>13.04</i>	0.02 <i>0.05</i>	1.3 <i>1.4</i>	11.78 <i>21.33</i>
Crops	0.9 <i>0.19</i>	8.14 <i>4.63</i>	0.19 <i>0.19</i>	27.35 <i>30.36</i>	16.62 <i>18.05</i>	26.38 <i>19.67</i>
Built area	2.75 <i>18.84</i>	44.41 <i>27.19</i>	28.43 <i>23.99</i>	23.8 <i>19.33</i>	33.06 <i>31.65</i>	18.14 <i>21.87</i>

Bare ground	0.2 <i>0.06</i>	0.16 <i>0.25</i>	0.2 <i>0.26</i>	0.09 <i>0.1</i>	0.1 <i>0.11</i>	1.35 <i>1.17</i>
Rangeland	19.22 <i>9.82</i>	7.75 <i>10.53</i>	9.24 <i>8.82</i>	6.96 <i>6.76</i>	17.39 <i>16.47</i>	39.22 <i>31.2</i>
Surface area and population estimates						
Top number: watershed scale						
<i>Bottom number: local scale (within 10 km of the monitoring sites)</i>						
Area (km ²)	11,703.6 <i>488.7</i>	1,392.8 <i>218.2</i>	921 <i>645.6</i>	523.8 <i>213.0</i>	114.05 <i>105.01</i>	378.16 <i>205.86</i>
Estimated population within the area (ppl)	167,164 <i>71,111</i>	670,180 <i>49,291</i>	288,031 <i>148,557</i>	58,937 <i>17,404</i>	49,622 <i>48,161</i>	134,972 <i>100,582</i>
Population density (ppl km ⁻²)	14 <i>145</i>	481 <i>225</i>	312 <i>230</i>	112 <i>81</i>	435 <i>458</i>	356 <i>488</i>
LULC definitions per Esri (see https://livingatlas.arcgis.com/landcover/)						
<p><i>Water</i> – areas where water was present throughout the year. Excludes man-made structures like docks</p> <p><i>Tree cover</i> – vegetation with closed/dense canopy ≥ 15 meters.</p> <p><i>Flooded vegetation</i> – areas with intermixing of water and vegetation flooded seasonally or predominantly throughout the year.</p> <p><i>Crops</i> – human planted vegetation (cereals, grasses, and corps) that are not at tree height.</p> <p><i>Built area</i> – human made structures like roads, rail road networks, parking spaces, industrial and residential buildings.</p>						

Bare ground – areas dominated by rocks, soil, sand (i.e. desert) with sparse to no vegetation throughout the year

Rangeland – homogeneous grasses, mixes of vegetation below tree-height with rocks and soil, clearings in the forests.

153

154 **Major precipitation events.**

155 To capture responses to precipitation events from years with contrasting annual
156 precipitation patterns, we selected comparatively wet and dry years for each estuary. Using
157 precipitation records from nearby airports we calculated a long-term interquartile range (IQR,
158 1990-2020) of total monthly precipitation for each estuary following Murrell et al. (2018).
159 Relatively wet/dry years were selected based on the number of months plotting above/below IQR
160 and total annual precipitation, while considering completeness of water quality, nutrient, and
161 meteorological data of each monitoring location (Fig. S1). Long-term precipitation records
162 included: Duluth International, Washington Reagan International, Jacksonville International,
163 Birmingham Airport, and San Francisco International airports (all available at:
164 <https://www.ncei.noaa.gov/cdo-web/datasets>). Further, we selected major precipitation events
165 within each wet and dry year by plotting daily precipitation using data from NERR
166 meteorological stations, which revealed clear outlier events for each estuary (Fig. S2). Individual
167 events were down-selected based on data availability at each monitoring location (event details
168 in Table S1).

169

170 **The resistance index.**

171 To understand and compare physicochemical factors and urban land-use characteristics
172 involved in estuarine responses to precipitation events, we calculated the resistance index
173 described in Orwin & Wardle (2004). Briefly, the index (range: +1 to -1) uses concentrations of a
174 response variable measured pre- and post-disturbance to represent system shift from an initial
175 condition (equation 1).

$$176 \quad \textit{Resistance} = 1 - \frac{2|D_0|}{(C_0 + |D_0|)} \quad (\text{eq. 1})$$

177

178 where, C_0 = concentration of the response variable pre-disturbance, and D_0 = difference between
179 the concentration of the response variable pre- and post-disturbance (P_0). An index value of +1
180 indicates maximum resistance. Index values between 0 and 1 show that $|D_0| \leq C_0$ (i.e., P_0 is
181 between 0 and $2C_0$). Resistance index of 0 indicates 100% decrease or increase in P_0 (i.e., $|D_0| =$
182 C_0), whereas index values between < 0 and -1 show that $|D_0| > C_0$ (i.e., $P_0 > 2C_0$). Overall, index
183 values below +1 indicate stronger effects of the disturbance and less resistant systems (Orwin &
184 Wardle, 2004).

185 Because DO measurements are widely available, and are often used as a proxy for water
186 quality, trophic state, and ecosystem metabolism (Caffrey, 2004; Mulholland et al., 2001;
187 Murrell et al., 2018; Odum, 1956), we used DO as the response variable in resistance
188 calculations. Because DO is impacted by temperature, salinity, and tidally induced advection, we
189 calculated C_0 as an average concentration within a timespan ≥ 24 hours
190 that was not affected by precipitation (Fig. S3, Table S1). Also, because the response time for
191 DO concentration following precipitation is not uniform across monitoring locations, the
192 timespan for estimating P_0 was selected in the context of the precipitation record for each event
193 as maximum displacement from C_0 within and past the event (Fig. S3, Table S1).

194

195 **Statistical analysis.**

196 *Linear Regression Analysis.* To test associations of specific physicochemical factors and
197 land-use characteristics with estuarine resistance to precipitation, we used linear regressions at
198 continental and local scales independently (i.e., all estuaries combined vs. within each individual
199 estuary) and within salinity-based groups (i.e., average annual salinity less than or above 10 ppt).
200 The ‘low salinity’ group included all monitoring locations at LKS and CBM, Fish River and
201 Middle Bay monitoring locations at WKB, and First Mallard and Second Mallard monitoring
202 locations at SFB. The ‘high salinity’ group included all monitoring locations at GTM, China
203 Camp and Gallinas Creek at SFB, and Weeks Bay at WKB during the dry year only. For
204 continental-scale and salinity-based regressions, the response variable was annual mean
205 resistance, regressed against mean annual physicochemical factors (i.e., water temperature, water
206 column depth, salinity, turbidity, DIN, PO_4^{-3} , and Chl-*a*.) for wet and dry years, respectively, and
207 LULC and population density as individual predictors. Annual means were used because of lack
208 of nutrient and Chl-*a* measurements surrounding selected precipitation events. Because of that,

209 regressions at each individual estuary (i.e. local-scale) also used annual mean resistance and
210 annual mean nutrient and Chl-*a* concentrations. However, local-scale regression analysis
211 involving water temperature, water column depth, salinity, and turbidity as individual predictors
212 of resistance used mean values calculated in the context of each precipitation event (see extent of
213 the event in Table S1), and the corresponding resistance values as response variables.

214 We did not include LULC and population density as predictors of resistance at individual
215 estuaries because of the close proximity of some monitoring locations to one another (< 800 m).
216 Comparative statistics within and between estuaries were conducted using Shapiro-Wilk
217 normality test followed by ANOVA with post-hoc Tukey HSD or Kruskal-Wallis test as
218 appropriate. Statistical analyses were performed in Python 3.10.11 using `scipy.stats`,
219 `statsmodels.stats.multicomp.pairwise_tukeyhsd`, and `seaborn.regplot` packages.

220

221 **Results**

222 **Land use/land cover and nutrient concentrations across estuaries.**

223 Using LULC and population density adjoining monitoring locations at each estuary, we
224 found that SFB was surrounded by predominantly urban-type land characteristics (e.g., built
225 area, population density) and that LKS had the lowest degree of urbanization (i.e., lowest
226 population density and highest percent tree cover) (Table 1). SFB San Pablo Bay (i.e., China
227 Camp and Gallinas Creek locations) had the largest percent built area (31.65 %), while SFB-
228 Suisun Bay (i.e., First Mallard and Second Mallard locations) had the highest population density
229 (448 ppl km⁻¹). Adjoining LULC at LKS was dominated by tree cover (58.78%). LULC
230 surrounding monitoring locations at CBM also had high percentages of tree cover (53.72%) and
231 built area (27.19%), with high population density (225 ppl km⁻²). Agricultural land was prevalent
232 at WKB (30.36%). Overall, SFB and CBM estuaries were characteristically more urbanized
233 compared to GTM and LKS estuaries. LULC breakdown and population density for all estuaries
234 on watershed level and adjacent to monitoring locations are shown in Table 1.

235 SFB and CBM had high DIN concentrations across both wet and dry years compared to
236 LKS and GTM (mean > 0.504 mg-N L⁻¹ versus mean < 0.16 mg-N L⁻¹, all $p < 0.01$, Fig. S4).
237 Phosphate concentrations were the highest at SFB (mean = 0.135 mg-P L⁻¹, all other means <
238 0.03 mg-P L⁻¹, $p < 0.001$, Fig. S4). Overall, mean N:P ratios across LKS, CBM, GTM, WKB,

239 and SFB estuaries were 28.04, 26.56, 2.84, 83.82, and 5.10, respectively (Fig. S5), with GTM
240 and SFB indicating N limiting conditions based on a 16N:1P Redfield ratio (Redfield, 1934).

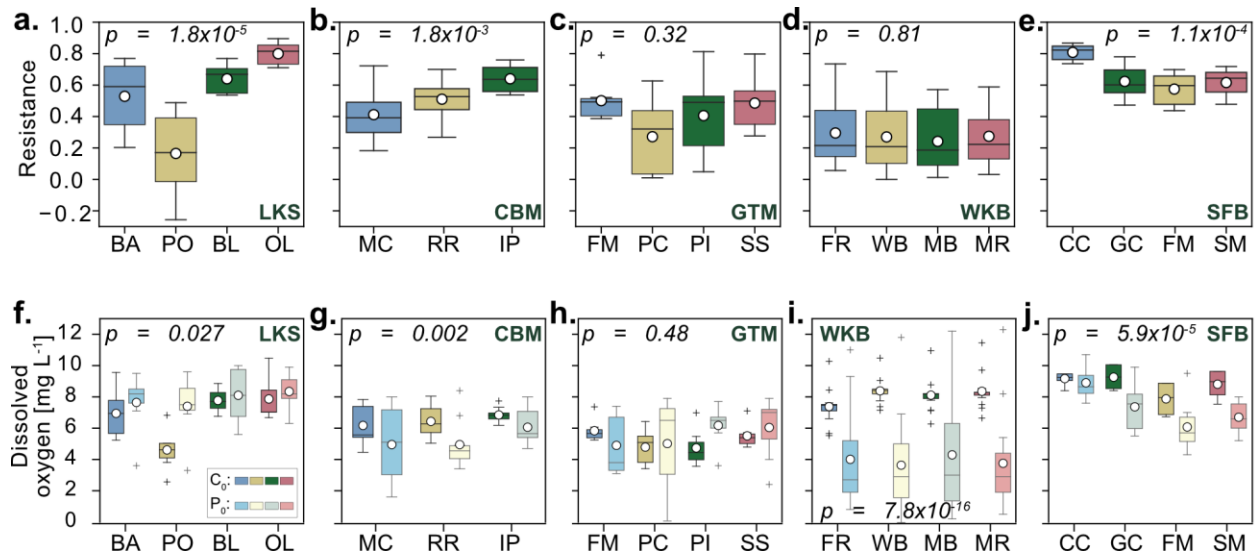
241

242 **Resistance to precipitation and changes in dissolved oxygen across estuaries and**
243 **monitoring locations.**

244 Resistance varied across all estuaries ($F = 21.6, p < 0.0001$, Fig. 2). SFB showed the
245 highest resistance (range of means: 0.56 - 0.81) while at LKS resistance reached some of the
246 lowest values (range of means: 0.30 - 0.64). Within individual estuaries (Fig. 2), resistance was
247 most variable at LKS ($F = 13.9, p < 0.0001$, the resistance index range: -0.26 - 0.89). At CBM,
248 resistance also varied across monitoring locations ($F = 7.9, p < 0.01$, range: 0.18 - 0.76).
249 Resistance values across GTM monitoring locations did not show significant differences ($F =$
250 $3.5, p = 0.32$, range: 0.01 - 0.81). Compared with other estuaries, resistance to precipitation
251 across WKB was most uniform, with no significant differences across WKB monitoring
252 locations ($F = 0.9, p = 0.81$, range: 0 - 0.73). Lastly, at SFB resistance values varied across the
253 estuary ($F = 10.2, p < 0.001$, range: 0.43 - 0.87).

254 DO concentrations pre- and post-precipitation varied across all estuaries ($C_0: F = 45.6, p$
255 $< 0.0001, P_0: F = 17.1, p < 0.0001$, Fig. 2). At SFB and CBM (i.e., more urban estuaries), DO
256 declined following precipitation (both $p < 0.01$). At LKS, precipitation events significantly
257 increased DO concentration ($F = 5.1, p = 0.027$). At WKB – an agriculture-dominated watershed
258 – DO decreased following precipitation as compared to its baseline concentration ($F = 86.9, p <$
259 0.0001). There was no significant difference between pre- and post-precipitation DO
260 concentrations at GTM ($F = 0.5, p = 0.48$).

261



262

263

264

265

266

267

268

269

270

271

272

273

274

275

276

277

278

279

280

281

282

283

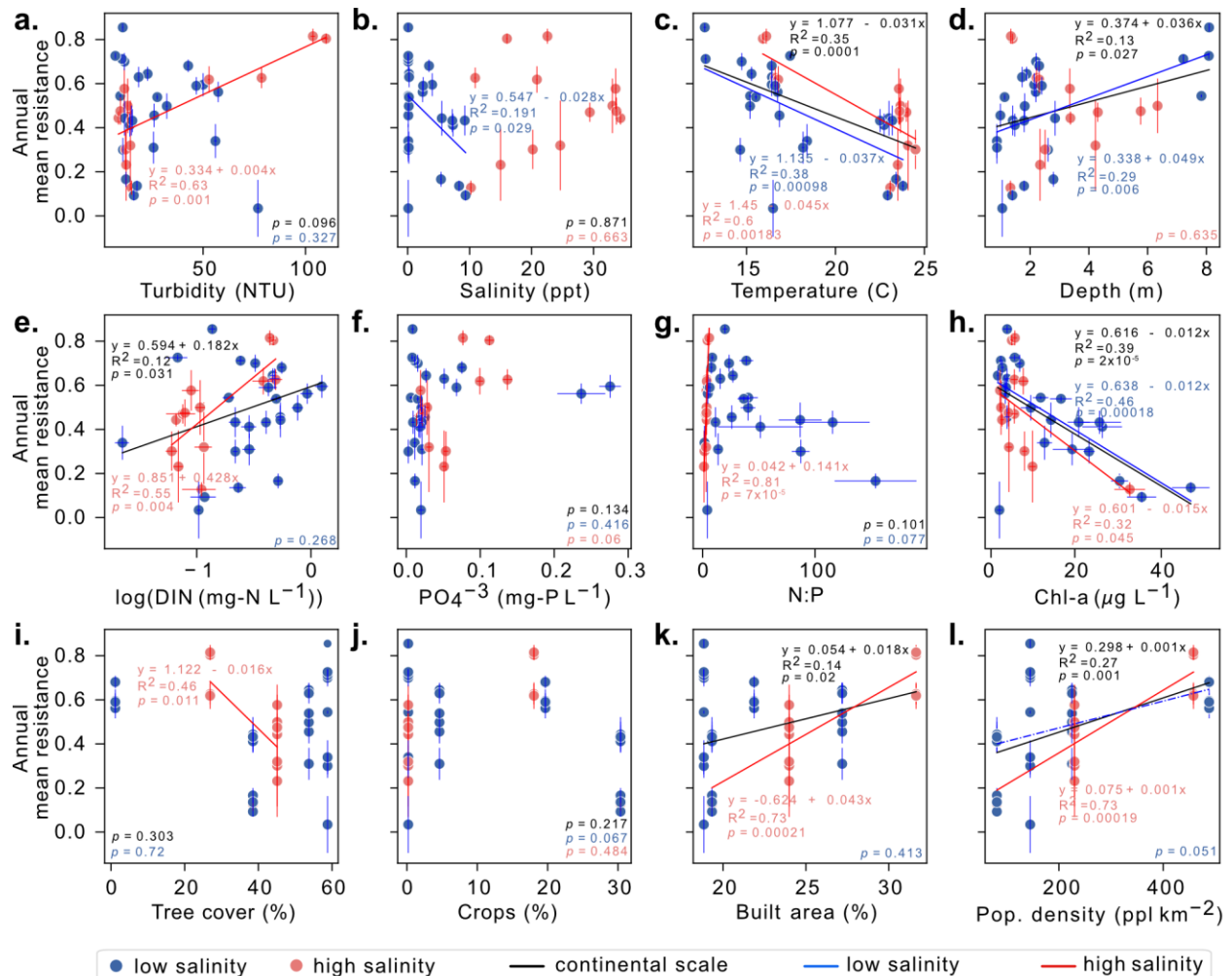
Fig. 2. Variation in resistance within individual estuaries with pre- and post-disturbance distribution of dissolved oxygen. Boxes show the quartiles of the dataset and the whiskers show the rest of the distribution. Means are shown in white circles, and medians are shown in black solid lines. *P*-values are at the top of each panel. a) Lake Superior (LKS) NERR (all $n = 7$). b) Chesapeake Bay (CBM) NERR (all $n = 10$). c) Guana Tolomato-Matanzas (GTM) NERR (all $n = 7$). d) Weeks Bay (WKB) NERR (all $n = 15$). e) San Francisco Bay (SFB) NERR ($n = 8$ except Second Mallard (SM) $n = 7$). f-j) Distribution of dissolved oxygen concentrations prior to (C_0 , darker shades) and post (P_0 , lighter shades) precipitation.

Cross-scale relationships of resistance with physicochemical factors, land use/land cover characteristics, and population density.

When data from the five estuaries were considered together (i.e., continental-scale), we found significant positive relationships of annual mean resistance to water column depth, DIN, percent built area, and population density; and significant negative relationships to water temperature and Chl-*a* (all: $p < 0.027$; $R^2 > 0.12$) (Fig. 3).

When grouped by salinity, estuarine resistance to precipitation was more tightly correlated to physicochemical factors and land-use characteristics (i.e., higher R^2) compared to continental-scale relationships (Fig. 3). Within ‘low-salinity’ estuaries, annual mean resistance was positively related to depth of the water column, which is consistent with the trend observed on continental-scale; and negatively related to annual mean salinity – a relationship not found on continental-scale (both: $p < 0.03$, $R^2 > 0.19$). Within ‘high-salinity’ estuaries – annual mean

284 resistance showed positive relationships to annual mean log(DIN) and to percent built area (both:
 285 $p < 0.005$, $R^2 > 0.54$), which also was consistent with continental-scale results. Observations
 286 present in ‘high-salinity’ estuaries but absent from continental-scale evaluations included
 287 negative relationships of annual mean resistance to tree cover, and negative relationships to N:P
 288 ratio and turbidity (all: $p < 0.012$, $R^2 > 0.45$). Additionally, annual mean resistance in both low-
 289 and high-salinity groups was positively related to population density, and negatively related to
 290 water temperature and Chl-*a* (all: $p < 0.0511$, $R^2 > 0.15$). The latter trends were consistent with
 291 continental-scale observations. Generally, ‘low-salinity’ estuaries showed fewer relationships of
 292 annual mean resistance to annual mean physicochemical factors, LULC, and population density
 293 compared to ‘high-salinity’ estuaries.



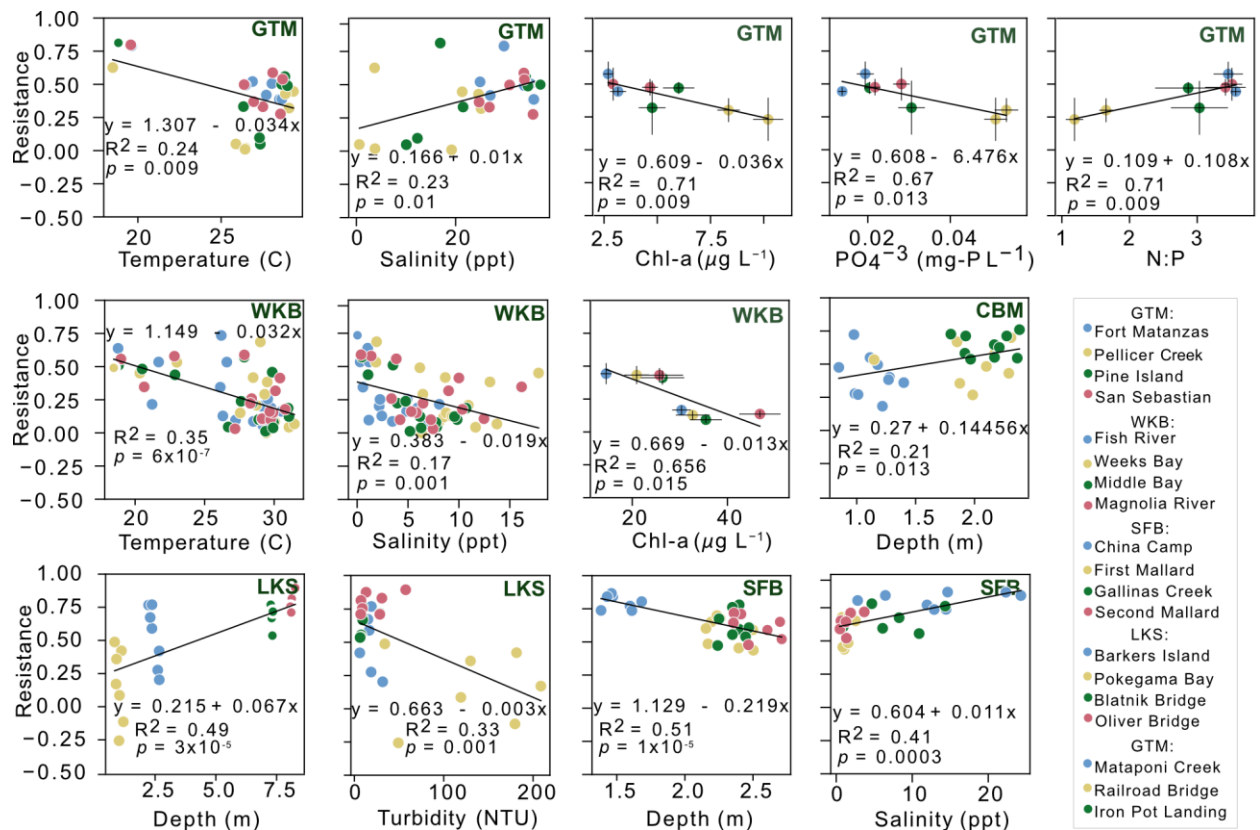
294

295 **Fig. 3.** Relationships of continental-scale and salinity-based resistance to physicochemical
 296 factors, land use/land cover, and population density. Continental-scale regressions considered
 297 all monitoring locations across all estuaries. Significant relationships ($p < 0.05$) are shown in

298 black, red, and blue for continental-scale, high-salinity estuaries, and low-salinity estuaries,
 299 respectively. Standard errors of the mean are shown in vertical and horizontal lines.

300

301 On local scales (i.e., within each estuary), resistance was related to some
 302 physicochemical factors that were not observed in continental-scale relationships. Moreover, the
 303 number, strength, and trends of relationships between local-scale resistance and physicochemical
 304 factors varied substantially across estuaries (Fig. 4, Figs. S7, S8). Resistance at GTM had the
 305 most relationships to physicochemical factors. It was negatively related to water temperature,
 306 PO_4^{3-} , and Chl-*a* concentrations; and positively related to salinity and N:P (all: $p < 0.014$, $R^2 >$
 307 0.23). In contrast, at CBM, the resistance was related only to water column depth (positive, $p =$
 308 0.013 , $R^2 = 0.21$). At LKS, resistance was positively related to water column depth, and
 309 negatively related to turbidity (both: $p < 0.002$, $R^2 > 0.32$). At WKB, relationships of resistance
 310 to water temperature, salinity, and Chl-*a* concentrations were all negative (all: $p < 0.015$, $R^2 >$
 311 0.16). At SFB, resistance was negatively related to water column depth, which opposed the
 312 general trend, and positively related to salinity (both: $p < 0.0004$, $R^2 > 0.40$).

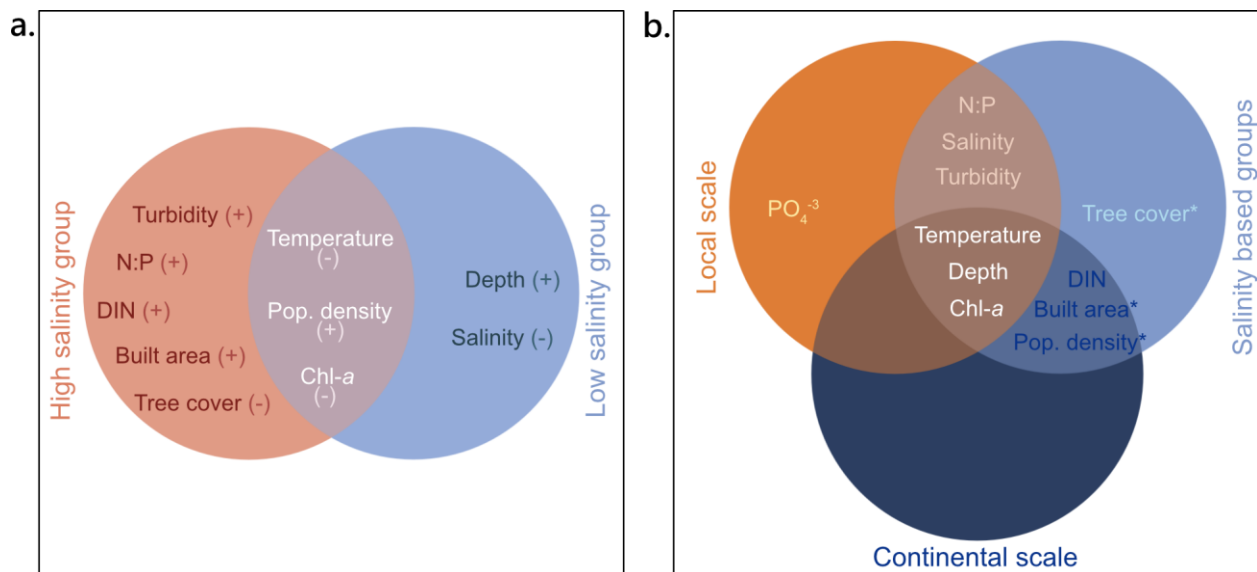


313

314 **Fig. 4.** Relationships between resistance and physicochemical factors for each estuary. National
315 Estuarine Reserve System (NERR) estuary abbreviations: Lake Superior (LKS) NERR,
316 Chesapeake Bay, Maryland (CBM) NERR, Guana Tolomato Matanzas (GTM) NERR, Weeks
317 Bay (WKB) NERR, and San Francisco Bay (SFB) NERR. Significant correlations ($p < 0.05$) are
318 shown with black lines. Standard errors of the mean are shown in vertical and horizontal lines for
319 relationships using annual means for predictor and response variables. For additional results see
320 Figs. S7 and S8.

321
322 Overall, we found that some relationships of resistance with physicochemical factors and
323 urban land-use characteristics appeared to be universal while others varied across scales (Fig. 5).
324 This included the uniquely identified relationships between resistance and PO_4^{-3} at GTM, and
325 resistance to tree cover found within ‘high-salinity’ estuaries. Cross-scale relationships of
326 resistance included: 1) positive relationships to N:P ratio, salinity (positive and negative), and
327 turbidity (positive), which were identified in both local-scale and salinity-based evaluations; 2)
328 relationships to $\log(\text{DIN})$, percent built area, and population density (all positive), which were
329 identified in continental-scale and salinity-based evaluations; and 3) relationships to water
330 temperature (negative), water column depth (positive and negative), and Chl-*a* (negative)
331 identified across continental- and local-scales, and within salinity-based estuary groups.

332



333

334 **Fig. 5.** Cross-scale relationships of estuarine resistance to physicochemical factors and land-
335 characteristics. a) Venn diagram of resistance relationships to physicochemical factors and land-

336 use characteristics in high- vs. low-salinity estuaries. Positive or
337 negative relationships are indicated with '+' and '-' respectively. b)
338 Venn diagram of resistance relationships with physicochemical factors and
339 land-use characteristics in continental, local, and salinity-based groups. Estuarine resistance to
340 land use/land cover and population density marked with asterisks (*) were not evaluated at local-
341 scale due to overlap in the spatial domains of some monitoring locations.

342

343 *Discussion*

344 Understanding patterns in estuarine responses to precipitation at continental-to-global
345 scale is important for predicting impacts of urbanization and climate change on estuarine
346 environments as a whole. However, the patterns identified at such large scales may not be
347 applicable when it comes to predicting estuarine behavior at local scales. As shown by previous
348 studies that focused on anthropogenic influences on streams and estuaries, contrasting
349 relationships between drivers and responses to disturbances are common for systems with
350 different climatic conditions, regional geology, and other ecosystem factors (Baker et al., 2004;
351 Gannon et al., 2022; Hopkins et al., 2015; Kaushal et al., 2018; Ombadi & Varadharajan, 2022;
352 Poff et al., 2006). Our results underscore the importance of cross-scale evaluations. We show
353 that while relationships between estuarine resistance, urbanization, and DIN may be overarching
354 dynamics at the continental-scale they may not relate to resistance on the estuary level. Local
355 resistance can be impacted by myriad factors that are different from factors identified at larger
356 scales. Also, in contrast to our overarching hypothesis, we find that urbanized estuaries tend to
357 have higher resistance than more pristine estuaries. These results suggest that the effects of
358 watershed urbanization could positively impact estuarine ecosystem stability by providing a
359 mechanism that allows estuaries responding to major precipitation events to withstand large
360 shifts in DO concentrations or quickly restore DO back to its baseline.

361

362 **Baseline and post-precipitation dissolved oxygen concentration vary across estuaries.**

363 Estuaries with urban (i.e., built area, population density) and agriculture-dominated
364 LULC, showed an overall decrease in DO concentrations after precipitation events (SFB, CBM,
365 and WKB: $p < 0.0001$, Fig. 2). This suggests that precipitation generally has a predominantly
366 negative effect on DO concentration in urbanized estuaries (i.e., SFB and CBM), and estuaries

367 surrounded by agricultural land (i.e., WKB). Simultaneously, at LKS – a less urbanized estuary,
368 post-precipitation DO concentrations increased ($F = 5.1$, $p = 0.027$, Fig. 2). No differences
369 between pre- and post-precipitation DO concentrations were found at GTM.

370 There are vast differences in geometry, circulation, and hydrologic conditions among
371 SFB, CBM, and WKS and yet, they exhibit similar DO concentration patterns. At the local-scale,
372 a wide range of physical factors can impact DO concentrations in estuaries including channel
373 geometry and river discharge (Kemp & Boynton, 1980; Raymond et al., 2012; Raymond & Cole,
374 2001), wind (Scully, 2010; Zheng et al., 2024), and circulation (Raimonet & Cloern, 2017).
375 Urban estuaries often serve as basins for wastewater treatment outflows which can supply
376 continued freshwater discharge and nutrients when river discharge is low. Both urban and
377 agriculturally influenced estuaries are prone to increased nutrient loading during and shortly after
378 precipitation events (Bernhardt et al., 2008; Walsh et al., 2005), which impacts primary
379 production and microbial metabolism and may lead to declines in DO concentrations.

380 Also, local controls on DO dynamics are likely different among SFB, CBM, and WKS
381 estuaries. In addition to being the most urban estuaries in our study, SFB and CBM are also the
382 largest and deepest. Therefore, at SFB and CBM, DO may be governed more heavily by physical
383 controls like circulation (Raimonet & Cloern, 2017) and wind (Zheng et al., 2024) in addition to
384 anthropogenic factors like wastewater discharge. In contrast, WKS is a small, shallow, and
385 highly productive estuary. Therefore, at WKB, DO may be more heavily governed by nutrient
386 loading that fosters primary production, and by rapid flushing during storm events (Novoveská,
387 2019). Differences in primary DO controls may help explain why estuaries with similar DO
388 concentration patterns have different resistance to precipitation.

389

390 **Urbanization and inorganic nitrogen correspond with elevated resistance to precipitation** 391 **at the continental-scale.**

392 The overall higher resistance values of the most urbanized estuaries and the overarching
393 relationships of urban LULC with resistance suggest that estuaries within urban watersheds may
394 be able to withstand and/or recover faster from major precipitation events (Fig. 3). This result
395 contradicts our overarching hypothesis that urban estuaries should show low resistance to
396 precipitation because of frequent physical and chemical disturbances, like flashiness, streambed
397 scouring, and N loading, which alter hydrology, turbidity, and interfere with stream metabolism

398 (Bernhardt et al., 2008; Groffman et al., 2004; Hession et al., 2003; Walsh et al., 2005).
399 However, anthropogenically induced physicochemical alterations may also increase estuarine
400 resistance to precipitation events. As such, it is possible that watershed urbanization could equip
401 estuaries with a set of controls that allow mitigation of processes that drive DO to extreme
402 concentrations, like algal blooms, which can induce large DO fluctuations in water by
403 overproducing DO during the day above saturation levels and severely depleting DO at night
404 (Chapin et al., 2004; Ni et al., 2020). For instance, an increase in flashiness would increase flow
405 velocity and reaeration of the water column (Raymond et al., 2012; Raymond & Cole, 2001), and
406 contribute to phytoplankton removal via transport or turbidity-driven light attenuation, which
407 limits phytoplankton growth (Caffrey, 2004; Pennock & Sharp, 1986). Turbidity-driven control
408 on phytoplankton was previously reported for SFB estuary (Cloern, 1987), despite N abundance.
409 Such control for overgrowth of phytoplankton would help maintain DO near baseline. We found
410 positive relationships of turbidity with percent built area and population density ($p < 0.00051$, R^2
411 > 0.28), and negative relationships of Chl-*a* with percent built area and population density ($p <$
412 0.02 , $R^2 > 0.14$) (Fig. S6).

413 Also, watershed urbanization is often related to high N export to freshwater, marine
414 environments, and estuaries (Bettez et al., 2015; Reisinger et al., 2016). We found that in
415 addition to urbanization, estuary N content was also a major predictor of resistance at the
416 continental-scale. While excess nutrients is a significant problem for urban aquatic environments
417 (Beman et al., 2005; Bernot et al., 2010; Black et al., 2011; Mulholland et al., 2008), appropriate
418 levels of N support basic metabolic functions across a wide range of systems and environmental
419 conditions (Camenzind et al., 2018; Howarth, 1988; Schimel & Bennett, 2004; Sullivan et al.,
420 2014; Q. Zhang et al., 2021). N plays a major role in phytoplankton growth in streams and
421 estuaries across urbanization gradient (Foldager Pedersen & Borum, 1996; Gobler et al., 2006;
422 Howarth & Marino, 2006; Larsen & Harvey, 2017; Moore & Hunt, 2013; Vitousek & Howarth,
423 1991; Woodland et al., 2015). This link between N availability and phytoplankton is important
424 because phytoplankton is a part of the DO delivery mechanism to aquatic systems, traditionally
425 incorporated in models for net ecosystem respiration as a gross primary production term (Odum,
426 1956). We found DIN concentrations to positively correlate with urban land characteristics (e.g.,
427 percent crops and population density; $p < 0.025$, $R^2 > 0.12$, Fig. S6) and with resistance at the
428 continental-scale ($p = 0.031$, $R^2 = 0.12$; Fig. 3).

429 Moreover, relationships of resistance with N and urbanization were particularly evident
430 in high-salinity estuaries. We found positive relationships of resistance with built area and N:P in
431 high-salinity estuaries and negative relationships between resistance and percent tree cover ($p <$
432 0.012 , $R^2 > 0.45$; Fig. 3). Nitrogen limitation occurs across a wide range of aquatic environments
433 and is particularly prevalent in marine systems (Elser et al., 2007; Guildford & Hecky, 2000;
434 Paerl, 2018; Paerl & Piehler, 2008). Additionally, a recent study suggests that riparian zones
435 have a high capacity to retain N concentrations in surface runoff and groundwater (Lyu et al.,
436 2021). In concert with N limitation that prevails in marine environments, N retention by riparian
437 zones can exacerbate N-limiting growth conditions in estuaries with high salinity, and
438 particularly for phytoplankton.

439

440 **Water column depth, temperature, and Chl-*a* relate to resistance across all scales.**

441 Across all scales, we found a generalizable pattern where resistance was often related to
442 water column depth (overall positive relationship), water temperature (negative relationship), and
443 concentration of phytoplankton (negative relationship) (Figs. 3-5). Urbanization-driven changes
444 to watershed LULC from forested to agriculture and infrastructure dominated landscapes, can
445 deepen the channel through processes like increased runoff and sediment transport, hydrological
446 flashiness, channel dredging, and/or other anthropogenic activities (O'Driscoll et al., 2010;
447 Simon & Rinaldi, 2006; Walsh et al., 2005). Generally, to induce similar shifts in ecosystem
448 resistance in relatively deep versus shallow streams or estuaries, the magnitude of the
449 disturbance should be proportional to the system's volume. Through dilution, deeper streams
450 have greater capacity to resist changes associated with precipitation that affect DO availability
451 like influx of oxygen-saturated rain water, nutrient loading, and turbulence and water-
452 atmosphere gas exchange. Also, channels can have an increased seasonal gross production rate
453 of DO compared to shoal sites (Murrell et al., 2018). Similarly, deeper streams have longer
454 equilibration time with environmental conditions and less diel variability in parameters like
455 temperature (Caissie, 2006; Macan, 1958), which affects diel and seasonal DO dynamics, likely
456 resulting in a tighter range in baseline DO.

457 Moreover, because temperature is a major control for various chemical and biological
458 processes known to impact DO availability in aquatic systems (e.g., microbial metabolic and
459 growth rates, oxygen solubility), many studies have focused on the impact of rising temperature

460 on DO dynamics in streams and estuaries (Apple et al., 2006; Caffrey, 2003; Caffrey et al.,
461 2014). Highlighted results link climate change and urbanization to thermal pollution of urban
462 streams following rain events (Zahn et al., 2021), and show connections of elevated global
463 temperatures with decreased primary production (Song et al., 2018) and increased planktonic N
464 demand (Toseland et al., 2013). Therefore, the combined effects of watershed urbanization and
465 global temperature increase on phytoplankton could exacerbate DO dynamics in estuaries and
466 significantly shift the range of DO baseline. We found a negative relationship between resistance
467 and water temperature across all analyses (Figs. 3, 4).

468 Finally, our results suggest that negative relationships between estuarine resistance to
469 precipitation and concentration of Chl-*a* may be generalizable features of estuaries (Figs. 3, 4).
470 This supports previous reports of DO deviations from baseline induced by excess phytoplankton
471 (Beman et al., 2005; Paerl, 2018; Wang & Zhang, 2020).

472

473 **Predictors of resistance on local scales vary across estuaries and differ from continental-** 474 **scale predictors.**

475 The contrasting relationships between physicochemical factors and resistance across
476 individual estuaries highlight substantial local scale variation (Fig. 4). For example, resistance at
477 CBM is related to one factor, water column depth, while at GTM, resistance is related to five
478 factors. This suggests that while water temperature, water column depth, and Chl-*a* may be
479 generalizable predictors for estuarine resistance at the continental scale, individual estuaries may
480 need to consider additional factors in water-quality management and conservation strategies. For
481 example, Chl-*a* and dissolved inorganic phosphorus have been shown to respond to storms in
482 some systems more than in others (Chen et al., 2015; N. G. Dix et al., 2008; Liao et al., 2021; M.
483 Zhang et al., 2022). This is because variability in controls on phytoplankton biomass on local
484 scales (i.e., light limitation, benthic and pelagic grazing, nutrient conditions, precipitation extent)
485 can influence Chl-*a* concentrations and its responses to storms (Cloern, 2001; Cloern & Jassby,
486 2010; N. Dix et al., 2013). Likewise, water temperature and salinity also vary in response to
487 storms in estuaries (Buelo et al., 2023; Chen et al., 2015; N. G. Dix et al., 2008), and were
488 previously identified as primary drivers of variability of biological processes and phytoplankton
489 activity across NERR estuaries (Apple et al., 2008). Moreover, seasonality and long-term

490 climatic conditions are known to change resistance to disturbances in aquatic systems (Beaulieu
491 et al., 2013; Reisinger et al., 2017; Van Meerbeek et al., 2021).

492 While there are myriad potential system-specific interactions that may result in different
493 responses to stressors, our results highlight that system-variability is important when identifying
494 parameters involved in ecosystem resistance to precipitation, which may or may not be reflected
495 in relationships and trends evaluated at the continental scale. We also acknowledge that other
496 scales of investigation (e.g., regional) could introduce additional insight into predictors of
497 estuarine resistance.

498

499 **Could N play a central role in increased resistance to precipitation in urban estuaries?**

500 Based on our findings that urban estuaries may be more resistant to precipitation than
501 more natural estuaries, we suggest that watershed urbanization may be accompanied by
502 adaptation mechanisms that help estuaries offset the effects of precipitation. In particular, we
503 hypothesize that hydrological flashiness and N delivery associated with precipitation can
504 influence phytoplankton and DO concentrations to have an overall positive effect on functional
505 stability in estuaries impacted by urbanization.

506 Dissolved oxygen availability in aquatic environments, including estuaries, is tightly
507 linked to phytoplankton, which in turn relies on adequate N availability (Evans & Seemann,
508 1989; Howarth, 1988; Vitousek & Howarth, 1991). This is particularly true for high-salinity
509 estuaries, which are often N-limited (Howarth & Marino, 2006; Paerl, 2018), and are
510 comparatively more restrictive for phytoplankton development because of growth-limiting salt
511 concentrations (Flameling & Kromkamp, 1994; Mo et al., 2021; Russell et al., 2023). However,
512 excess phytoplankton growth, often referred to as algal blooms, still occurs, even in high-salinity
513 estuaries (Anderson et al., 2021). Also, because watershed urbanization is often accompanied by
514 increased flashiness during rain events (B. K. Smith & Smith, 2015), it follows that precipitation
515 may rapidly remove phytoplankton through increased flow velocity. Storm runoff may also
516 simultaneously deliver necessary N concentrations that help phytoplankton biomass recover and
517 restore baseline DO concentrations in urban estuaries, where N loadings tend to be higher
518 (Bettez et al., 2015; Reisinger et al., 2016). Collectively, these processes could lead to higher
519 resistance to precipitation in urban estuaries that may be more responsive to N inputs. However,
520 we note that high-resolution measurements surrounding precipitation events, as well as careful

521 evaluations of phytoplankton, salinity, and N surrounding the events are needed to distinguish
522 effects on DO concentrations pre- and post-precipitation. We also highlight the importance of
523 evaluating N as species, because of known inhibitory effects of excess ammonium on nitrate
524 uptake by phytoplankton, which reduces the likelihood of algal blooms (Dugdale et al., 2007;
525 Parker et al., 2012).

526

527 ***Conclusions***

528 In light of emerging climatic and urban scenarios, cross-scale evaluations of parameters involved
529 in system responses to perturbations are important when considering management strategies for
530 water quality suitable for continental and local-scales. We found that (1) urban estuaries are
531 more resistant to precipitation; and (2) depth of the water column, water temperature, and Chl-*a*
532 are generalizable cross-scale predictors for estuarine resistance. However, across different scales,
533 we found that system-variability, including salinity, can interfere with the generalizable patterns
534 and result in additional relationships between resistance and physicochemical factors and land-
535 use characteristics. We also propose a hypothesis that urban estuaries may have adaptation
536 mechanisms that help DO resist the combined effects of watershed urbanization and major
537 precipitation events. However, high-resolution water quality and nutrient data surrounding
538 precipitation events, as well as models for system responses to precipitation, are needed to help
539 elucidate the underlying mechanisms for high resistance of urban estuaries.

540

541 ***Acknowledgements***

542 This material is based upon work supported by the U.S. Department of Energy, Office of
543 Science, Biological and Environmental Research program Early Career award to EBG. The work
544 was performed by Pacific Northwest National Laboratory, operated by Battelle Memorial
545 Institute for the U.S. Department of Energy under Contract DE-AC05-76RL01830. We thank the
546 National Estuarine Research Reserve System (NERRS), supported by awards from the Office for
547 Coastal Management, National Oceanographic and Atmospheric Administration (NOAA), and
548 Drs. Kyle Derby and Scott Phipps from Chesapeake Bay, Maryland NERR and Weeks Bay
549 NERR, respectively, for maintaining water quality monitoring stations and providing publicly
550 available data upon which this publication is based. The authors report no conflicts of interests.

551

553 **References**

- 554 Anderson, D. M., Fensin, E., Gobler, C. J., Hoeglund, A. E., Hubbard, K. A., Kulis, D. M.,
555 Landsberg, J. H., Lefebvre, K. A., Provoost, P., Richlen, M. L., Smith, J. L., Solow, A. R.,
556 & Trainer, V. L. (2021). Marine harmful algal blooms (HABs) in the United States:
557 History, current status and future trends. *Harmful Algae*, 102, 101975.
558 <https://doi.org/10.1016/j.hal.2021.101975>
- 559 Apple, J. K., Giorgio, P. A. del, & Kemp, W. M. (2006). Temperature regulation of bacterial
560 production, respiration, and growth efficiency in a temperate salt-marsh estuary. *Aquatic*
561 *Microbial Ecology*, 43(3), 243–254. <https://doi.org/10.3354/ame043243>
- 562 Apple, J. K., Smith, E. M., & Boyd, T. J. (2008). Temperature, Salinity, Nutrients, and the
563 Covariation of Bacterial Production and Chlorophyll-a in Estuarine Ecosystems. *Journal*
564 *of Coastal Research*, 2008(10055), 59–75. <https://doi.org/10.2112/SI55-005.1>
- 565 Baker, D. B., Richards, R. P., Loftus, T. T., & Kramer, J. W. (2004). A New Flashiness Index:
566 Characteristics and Applications to Midwestern Rivers and Streams1. *JAWRA Journal of*
567 *the American Water Resources Association*, 40(2), 503–522.
568 <https://doi.org/10.1111/j.1752-1688.2004.tb01046.x>
- 569 Beaulieu, J. J., Arango, C. P., Balz, D. A., & Shuster, W. D. (2013). Continuous monitoring
570 reveals multiple controls on ecosystem metabolism in a suburban stream. *Freshwater*
571 *Biology*, 58(5), 918–937. <https://doi.org/10.1111/fwb.12097>
- 572 Beman, M. J., Arrigo, K. R., & Matson, P. A. (2005). Agricultural runoff fuels large phytoplankton
573 blooms in vulnerable areas of the ocean. *Nature*, 434(7030), Article 7030.
574 <https://doi.org/10.1038/nature03370>
- 575 Bernhardt, E. S., Band, L. E., Walsh, C. J., & Berke, P. E. (2008). Understanding, Managing,
576 and Minimizing Urban Impacts on Surface Water Nitrogen Loading. *Annals of the New*
577 *York Academy of Sciences*, 1134, 61–96. <https://doi.org/10.1196/annals.1439.014>
- 578 Bernot, M. J., Sobota, D. J., Hall Jr, R. O., Mulholland, P. J., Dodds, W. K., Webster, J. R.,
579 Tank, J. L., Ashkenas, L. R., Cooper, L. W., Dahm, C. N., Gregory, S. V., Grimm, N. B.,
580 Hamilton, S. K., Johnson, S. L., Mcdowell, W. H., Meyer, J. L., Peterson, B., Poole, G.
581 C., Valett, H. M., ... Wilson, K. (2010). Inter-regional comparison of land-use effects on
582 stream metabolism. *Freshwater Biology*, 55(9), 1874–1890.
583 <https://doi.org/10.1111/j.1365-2427.2010.02422.x>
- 584 Bettez, N. D., Duncan, J. M., Groffman, P. M., Band, L. E., O'neil-dunne, J., Kaushal, S. S., Belt,
585 K. T., & Law, N. (2015). Climate Variation Overwhelms Efforts to Reduce Nitrogen
586 Delivery to Coastal Waters. *Ecosystems*, 18(8), 1319–1331.

- 587 <https://doi.org/10.1007/s10021-015-9902-9>
- 588 Bianchi, T. S. (2007). *Biogeochemistry of Estuaries*. Oxford University Press, USA.
- 589 Black, R. W., Moran, P. W., & Frankforter, J. D. (2011). Response of algal metrics to nutrients
590 and physical factors and identification of nutrient thresholds in agricultural streams.
591 *Environmental Monitoring and Assessment*, 175(1), 397–417.
592 <https://doi.org/10.1007/s10661-010-1539-8>
- 593 Bondarenko, M., Kerr, D., Sorichetta, A., & Tatem, A. (2020). *Census/projection-disaggregated*
594 *gridded population datasets for 189 countries in 2020 using Built-Settlement Growth*
595 *Model (BSGM) outputs* [dataset]. University of Southampton.
596 <https://doi.org/10.5258/SOTON/WP00684>
- 597 Booth, D. B., & Jackson, C. R. (1997). Urbanization of Aquatic Systems: Degradation
598 Thresholds, Stormwater Detection, and the Limits of Mitigation¹. *JAWRA Journal of the*
599 *American Water Resources Association*, 33(5), 1077–1090.
600 <https://doi.org/10.1111/j.1752-1688.1997.tb04126.x>
- 601 Buelo, C. D., Besterman, A. F., Walter, J. A., Pace, M. L., Ha, D. T., & Tassone, S. J. (2023).
602 Quantifying Disturbance and Recovery in Estuaries: Tropical Cyclones and High-
603 Frequency Measures of Oxygen and Salinity. *Estuaries and Coasts*.
604 <https://doi.org/10.1007/s12237-023-01255-1>
- 605 Caffrey, J. M. (2003). Production, Respiration and Net Ecosystem Metabolism in U.S. Estuaries.
606 In B. D. Melzian, V. Engle, M. McAlister, S. Sandhu, & L. K. Eads (Eds.), *Coastal*
607 *Monitoring through Partnerships: Proceedings of the Fifth Symposium on the*
608 *Environmental Monitoring and Assessment Program (EMAP) Pensacola Beach, FL,*
609 *U.S.A., April 24–27, 2001* (pp. 207–219). Springer Netherlands.
610 https://doi.org/10.1007/978-94-017-0299-7_19
- 611 Caffrey, J. M. (2004). Factors controlling net ecosystem metabolism in U.S. estuaries.
612 *Estuaries*, 27(1), 90–101. <https://doi.org/10.1007/BF02803563>
- 613 Caffrey, J. M., Murrell, M. C., Amacker, K. S., Harper, J. W., Phipps, S., & Woodrey, M. S.
614 (2014). Seasonal and Inter-annual Patterns in Primary Production, Respiration, and Net
615 Ecosystem Metabolism in Three Estuaries in the Northeast Gulf of Mexico. *Estuaries*
616 *and Coasts*, 37(1), 222–241. <https://doi.org/10.1007/s12237-013-9701-5>
- 617 Caissie, D. (2006). The thermal regime of rivers: A review. *Freshwater Biology*, 51(8), 1389–
618 1406. <https://doi.org/10.1111/j.1365-2427.2006.01597.x>
- 619 Camenzind, T., Hättenschwiler, S., Treseder, K. K., Lehmann, A., & Rillig, M. C. (2018). Nutrient
620 limitation of soil microbial processes in tropical forests. *Ecological Monographs*, 88(1),

- 621 4–21. <https://doi.org/10.1002/ecm.1279>
- 622 Chapin, T. P., Caffrey, J. M., Jannasch, H. W., Coletti, L. J., Haskins, J. C., & Johnson, K. S.
623 (2004). Nitrate sources and sinks in Elkhorn Slough, California: Results from long-term
624 continuous in situ nitrate analyzers. *Estuaries*, 27(5), 882–894.
625 <https://doi.org/10.1007/BF02912049>
- 626 Chen, N., Wu, Y., Chen, Z., & Hong, H. (2015). Phosphorus export during storm events from a
627 human perturbed watershed, southeast China: Implications for coastal ecology.
628 *Estuarine, Coastal and Shelf Science*, 166, 178–188.
629 <https://doi.org/10.1016/j.ecss.2015.03.023>
- 630 Cloern, J. E. (1987). Turbidity as a control on phytoplankton biomass and productivity in
631 estuaries. *Continental Shelf Research*, 7(11), 1367–1381. [https://doi.org/10.1016/0278-](https://doi.org/10.1016/0278-4343(87)90042-2)
632 [4343\(87\)90042-2](https://doi.org/10.1016/0278-4343(87)90042-2)
- 633 Cloern, J. E. (2001). Our evolving conceptual model of the coastal eutrophication problem.
634 *Marine Ecology Progress Series*, 210, 223–253. <https://doi.org/10.3354/meps210223>
- 635 Cloern, J. E., & Jassby, A. D. (2010). Patterns and Scales of Phytoplankton Variability in
636 Estuarine–Coastal Ecosystems. *Estuaries and Coasts*, 33(2), 230–241.
637 <https://doi.org/10.1007/s12237-009-9195-3>
- 638 Dix, N. G., Philips, E. J., & Gleeson, R. A. (2008). Water Quality Changes in the Guana
639 Tolomato Matanzas National Estuarine Research Reserve, Florida, Associated with Four
640 Tropical Storms. *Journal of Coastal Research*, 2008(10055), 26–37.
641 <https://doi.org/10.2112/SI55-008.1>
- 642 Dix, N., Philips, E., & Suscy, P. (2013). Factors Controlling Phytoplankton Biomass in a
643 Subtropical Coastal Lagoon: Relative Scales of Influence. *Estuaries and Coasts*, 36(5),
644 981–996. <https://doi.org/10.1007/s12237-013-9613-4>
- 645 Dugdale, R. C., Wilkerson, F. P., Hogue, V. E., & Marchi, A. (2007). The role of ammonium and
646 nitrate in spring bloom development in San Francisco Bay. *Estuarine, Coastal and Shelf*
647 *Science*, 73(1), 17–29. <https://doi.org/10.1016/j.ecss.2006.12.008>
- 648 Elser, J. J., Bracken, M. E. S., Cleland, E. E., Gruner, D. S., Harpole, W. S., Hillebrand, H.,
649 Ngai, J. T., Seabloom, E. W., Shurin, J. B., & Smith, J. E. (2007). Global analysis of
650 nitrogen and phosphorus limitation of primary producers in freshwater, marine and
651 terrestrial ecosystems. *Ecology Letters*, 10(12), 1135–1142.
652 <https://doi.org/10.1111/j.1461-0248.2007.01113.x>
- 653 Evans, J. R., & Seemann, J. R. (1989). The allocation of protein nitrogen in the photosynthetic
654 apparatus: Costs, consequences, and control. In W. R. Briggs (Ed.), *Photosynthesis* (pp.

- 655 183–205). Alan R. Liss.
- 656 Fisher, S. G., Gray, L. J., Grimm, N. B., & Busch, D. E. (1982). Temporal Succession in a
657 Desert Stream Ecosystem Following Flash Flooding. *Ecological Monographs*, 52(1), 93–
658 110. <https://doi.org/10.2307/2937346>
- 659 Flaming, I. A., & Kromkamp, J. (1994). Responses of respiration and photosynthesis of
660 *Scenedesmus protuberans* Fritsch to gradual and steep salinity increases. *Journal of*
661 *Plankton Research*, 16(12), 1781–1791. <https://doi.org/10.1093/plankt/16.12.1781>
- 662 Foldager Pedersen, M., & Borum, J. (1996). Nutrient control of algal growth in estuarine waters.
663 Nutrient limitation and the importance of nitrogen requirements and nitrogen storage
664 among phytoplankton and species of macroalgae. *Marine Ecology Progress Series*, 142,
665 261–272. <https://doi.org/10.3354/meps142261>
- 666 Gannon, J. P., Kelleher, C., & Zimmer, M. (2022). Controls on watershed flashiness across the
667 continental US. *Journal of Hydrology*, 609, 127713.
668 <https://doi.org/10.1016/j.jhydrol.2022.127713>
- 669 Gobler, C. J., Buck, N. J., Sieracki, M. E., & Sañudo-Wilhelmy, S. A. (2006). Nitrogen and
670 silicon limitation of phytoplankton communities across an urban estuary: The East River-
671 Long Island Sound system. *Estuarine, Coastal and Shelf Science*, 68(1), 127–138.
672 <https://doi.org/10.1016/j.ecss.2006.02.001>
- 673 Gregory, K. J. (2011). Wolman MG (1967) A cycle of sedimentation and erosion in urban river
674 channels. *Geografiska Annaler* 49A: 385-395. *Progress in Physical Geography*, 35(6),
675 831–841. <https://doi.org/10.1177/0309133311414527>
- 676 Grimm, N. B., Faeth, S. H., Golubiewski, N. E., Redman, C. L., Wu, J., Bai, X., & Briggs, J. M.
677 (2008). Global Change and the Ecology of Cities. *Science*, 319(5864), 756–760.
- 678 Groffman, P. M., Law, N. L., Belt, K. T., Band, L. E., & Fisher, G. T. (2004). Nitrogen Fluxes and
679 Retention in Urban Watershed Ecosystems. *Ecosystems*, 7(4), 393–403.
680 <https://doi.org/10.1007/s10021-003-0039-x>
- 681 Guildford, S. J., & Hecky, R. E. (2000). Total nitrogen, total phosphorus, and nutrient limitation
682 in lakes and oceans: Is there a common relationship? *Limnology and Oceanography*,
683 45(6), 1213–1223. <https://doi.org/10.4319/lo.2000.45.6.1213>
- 684 He, Q., & Silliman, B. R. (2019). Climate Change, Human Impacts, and Coastal Ecosystems in
685 the Anthropocene. *Current Biology*, 29(19), R1021–R1035.
686 <https://doi.org/10.1016/j.cub.2019.08.042>
- 687 Hession, W. C., Pizzuto, J. E., Johnson, T. E., & Horwitz, R. J. (2003). Influence of bank
688 vegetation on channel morphology in rural and urban watersheds. *Geology*, 31(2), 147–

- 689 150. [https://doi.org/10.1130/0091-7613\(2003\)031<0147:IOBVOC>2.0.CO;2](https://doi.org/10.1130/0091-7613(2003)031<0147:IOBVOC>2.0.CO;2)
- 690 Hopkins, K. G., Morse, N. B., Bain, D. J., Bettez, N. D., Grimm, N. B., Morse, J. L., Palta, M. M.,
691 Shuster, W. D., Bratt, A. R., & Suchy, A. K. (2015). Assessment of Regional Variation in
692 Streamflow Responses to Urbanization and the Persistence of Physiography.
693 *Environmental Science & Technology*, 49(5), 2724–2732.
694 <https://doi.org/10.1021/es505389y>
- 695 Howarth, R. W. (1988). Nutrient Limitation of Net Primary Production in Marine Ecosystems.
696 *Annual Review of Ecology and Systematics*, 19, 89–110.
- 697 Howarth, R. W., & Marino, R. (2006). Nitrogen as the limiting nutrient for eutrophication in
698 coastal marine ecosystems: Evolving views over three decades. *Limnology and*
699 *Oceanography*, 51(1part2), 364–376. https://doi.org/10.4319/lo.2006.51.1_part_2.0364
- 700 Kaushal, S. S., Likens, G. E., Pace, M. L., Utz, R. M., Haq, S., Gorman, J., & Grese, M. (2018).
701 Freshwater salinization syndrome on a continental scale. *Proceedings of the National*
702 *Academy of Sciences*, 115(4), E574–E583. <https://doi.org/10.1073/pnas.1711234115>
- 703 Kemp, W. M., & Boynton, W. R. (1980). Influence of biological and physical processes on
704 dissolved oxygen dynamics in an estuarine system: Implications for measurement of
705 community metabolism. *Estuarine and Coastal Marine Science*, 11(4), 407–431.
706 [https://doi.org/10.1016/S0302-3524\(80\)80065-X](https://doi.org/10.1016/S0302-3524(80)80065-X)
- 707 Kemp, W. M., Testa, J. M., Conley, D. J., Gilbert, D., & Hagy, J. D. (2009). Temporal responses
708 of coastal hypoxia to nutrient loading and physical controls. *Biogeosciences*, 6(12),
709 2985–3008. <https://doi.org/10.5194/bg-6-2985-2009>
- 710 Kyzar, T., Safak, I., Cebrian, J., Clark, M. W., Dix, N., Dietz, K., Gittman, R. K., Jaeger, J.,
711 Radabaugh, K. R., Roddenberry, A., Smith, C. S., Sparks, E. L., Stone, B., Sundin, G.,
712 Taubler, M., & Angelini, C. (2021). Challenges and opportunities for sustaining coastal
713 wetlands and oyster reefs in the southeastern United States. *Journal of Environmental*
714 *Management*, 296, 113178. <https://doi.org/10.1016/j.jenvman.2021.113178>
- 715 Larsen, L. G., & Harvey, J. W. (2017). Disrupted carbon cycling in restored and unrestored
716 urban streams: Critical timescales and controls. *Limnology and Oceanography*, 62(S1),
717 S160–S182. <https://doi.org/10.1002/lno.10613>
- 718 Leopold, L. B. (1968). Hydrology for urban land planning—A guidebook on the hydrologic
719 effects of urban land use. In *Circular* (554). U.S. Geological Survey.
720 <https://doi.org/10.3133/cir554>
- 721 Li, C., Zwiers, F., Zhang, X., Chen, G., Lu, J., Li, G., Norris, J., Tan, Y., Sun, Y., & Liu, M.
722 (2019). Larger Increases in More Extreme Local Precipitation Events as Climate Warms.

- 723 *Geophysical Research Letters*, 46(12), 6885–6891.
724 <https://doi.org/10.1029/2019GL082908>
- 725 Liao, A., Han, D., Song, X., & Yang, S. (2021). Impacts of storm events on chlorophyll-a
726 variations and controlling factors for algal bloom in a river receiving reclaimed water.
727 *Journal of Environmental Management*, 297, 113376.
728 <https://doi.org/10.1016/j.jenvman.2021.113376>
- 729 Lyu, C., Li, X., Yuan, P., Song, Y., Gao, H., Liu, X., Liu, R., & Yu, H. (2021). Nitrogen retention
730 effect of riparian zones in agricultural areas: A meta-analysis. *Journal of Cleaner*
731 *Production*, 315, 128143. <https://doi.org/10.1016/j.jclepro.2021.128143>
- 732 Macan, T. T. (1958). The temperature of a small stony stream. *Hydrobiologia*, 12(2), 89–106.
733 <https://doi.org/10.1007/BF00034143>
- 734 Martínez, M. L., Intralawan, A., Vázquez, G., Pérez-Maqueo, O., Sutton, P., & Landgrave, R.
735 (2007). The coasts of our world: Ecological, economic and social importance. *Ecological*
736 *Economics*, 63(2–3), 254–272. <https://doi.org/10.1016/j.ecolecon.2006.10.022>
- 737 Mo, Y., Peng, F., Gao, X., Xiao, P., Logares, R., Jeppesen, E., Ren, K., Xue, Y., & Yang, J.
738 (2021). Low shifts in salinity determined assembly processes and network stability of
739 microeukaryotic plankton communities in a subtropical urban reservoir. *Microbiome*,
740 9(1), 128. <https://doi.org/10.1186/s40168-021-01079-w>
- 741 Moore, T. L. C., & Hunt, W. F. (2013). Predicting the carbon footprint of urban stormwater
742 infrastructure. *Ecological Engineering*, 58, 44–51.
743 <https://doi.org/10.1016/j.ecoleng.2013.06.021>
- 744 Mulholland, P. J., Fellows, C. S., Tank, J. L., Grimm, N. B., Webster, J. R., Hamilton, S. K.,
745 Martí, E., Ashkenas, L., Bowden, W. B., Dodds, W. K., McDowell, W. H., Paul, M. J., &
746 Peterson, B. J. (2001). Inter-biome comparison of factors controlling stream metabolism.
747 *Freshwater Biology*, 46(11), 1503–1517. [https://doi.org/10.1046/j.1365-](https://doi.org/10.1046/j.1365-2427.2001.00773.x)
748 [2427.2001.00773.x](https://doi.org/10.1046/j.1365-2427.2001.00773.x)
- 749 Mulholland, P. J., Helton, A. M., Poole, G. C., Hall, R. O., Hamilton, S. K., Peterson, B. J., Tank,
750 J. L., Ashkenas, L. R., Cooper, L. W., Dahm, C. N., Dodds, W. K., Findlay, S. E. G.,
751 Gregory, S. V., Grimm, N. B., Johnson, S. L., McDowell, W. H., Meyer, J. L., Valett, H.
752 M., Webster, J. R., ... Thomas, S. M. (2008). Stream denitrification across biomes and
753 its response to anthropogenic nitrate loading. *Nature*, 452(7184), Article 7184.
754 <https://doi.org/10.1038/nature06686>
- 755 Murrell, M. C., Caffrey, J. M., Marcovich, D. T., Beck, M. W., Jarvis, B. M., & Hagy, J. D. (2018).
756 Seasonal oxygen dynamics in a warm temperate estuary: Effects of hydrologic variability

- 757 on measurements of primary production, respiration, and net metabolism. *Estuaries and*
758 *Coasts : Journal of the Estuarine Research Federation*, 41(3), 690–707.
759 <https://doi.org/10.1007/s12237-017-0328-9>
- 760 NERRS. (2023). *NOAA National Estuarine Research Reserve System (NERRS). System-wide*
761 *Monitoring Program*. <https://cdmo.baruch.sc.edu/>
- 762 Ni, W., Li, M., & Testa, J. M. (2020). Discerning effects of warming, sea level rise and nutrient
763 management on long-term hypoxia trends in Chesapeake Bay. *Science of The Total*
764 *Environment*, 737, 139717. <https://doi.org/10.1016/j.scitotenv.2020.139717>
- 765 Novoveská, L. (2019). Study of the seasonality and hydrology as drivers of phytoplankton
766 abundance and composition in a shallow estuary, Weeks Bay, Alabama (USA). *Journal*
767 *of Aquaculture & Marine Biology*, 8(3). <https://doi.org/10.15406/jamb.2019.08.00245>
- 768 O'Driscoll, M., Clinton, S., Jefferson, A., Manda, A., & McMillan, S. (2010). Urbanization Effects
769 on Watershed Hydrology and In-Stream Processes in the Southern United States.
770 *Water*, 2(3), Article 3. <https://doi.org/10.3390/w2030605>
- 771 Odum, H. T. (1956). Primary Production in Flowing Waters. *Limnology and Oceanography*, 1(2),
772 102–117. <https://doi.org/10.4319/lo.1956.1.2.0102>
- 773 Ombadi, M., & Varadharajan, C. (2022). Urbanization and aridity mediate distinct salinity
774 response to floods in rivers and streams across the contiguous United States. *Water*
775 *Research*, 220, 118664. <https://doi.org/10.1016/j.watres.2022.118664>
- 776 Orwin, K. H., & Wardle, D. A. (2004). New indices for quantifying the resistance and resilience
777 of soil biota to exogenous disturbances. *Soil Biology and Biochemistry*, 36(11), 1907–
778 1912. <https://doi.org/10.1016/j.soilbio.2004.04.036>
- 779 Paerl, H. W. (2018). Why does N-limitation persist in the world's marine waters? *Marine*
780 *Chemistry*, 206, 1–6. <https://doi.org/10.1016/j.marchem.2018.09.001>
- 781 Paerl, H. W., & Piehler, M. F. (2008). Chapter 11—Nitrogen and Marine Eutrophication. In D. G.
782 Capone, D. A. Bronk, M. R. Mulholland, & E. J. Carpenter (Eds.), *Nitrogen in the Marine*
783 *Environment (Second Edition)* (pp. 529–567). Academic Press.
784 <https://doi.org/10.1016/B978-0-12-372522-6.00011-6>
- 785 Parker, A. E., Hogue, V. E., Wilkerson, F. P., & Dugdale, R. C. (2012). The effect of inorganic
786 nitrogen speciation on primary production in the San Francisco Estuary. *Estuarine,*
787 *Coastal and Shelf Science*, 104–105, 91–101. <https://doi.org/10.1016/j.ecss.2012.04.001>
- 788 Pennock, J. R., & Sharp, J. H. (1986). Phytoplankton production in the Delaware Estuary:
789 Temporal and spatial variability. *Marine Ecology Progress Series*, 34(1/2), 143–155.
- 790 Pickett, S. T. A., Cadenasso, M. L., Grove, J. M., Boone, C. G., Groffman, P. M., Irwin, E.,

- 791 Kaushal, S. S., Marshall, V., McGrath, B. P., Nilon, C. H., Pouyat, R. V., Szlavecz, K.,
792 Troy, A., & Warren, P. (2011). Urban ecological systems: Scientific foundations and a
793 decade of progress. *Journal of Environmental Management*, 92(3), 331–362.
794 <https://doi.org/10.1016/j.jenvman.2010.08.022>
- 795 Poff, N. L., Bledsoe, B. P., & Cuhacyan, C. O. (2006). Hydrologic variation with land use across
796 the contiguous United States: Geomorphic and ecological consequences for stream
797 ecosystems. *Geomorphology*, 79(3), 264–285.
798 <https://doi.org/10.1016/j.geomorph.2006.06.032>
- 799 QGIS Development Team. (2023). *QGIS Geographic Information System*.
800 <https://www.qgis.org/en/site/>
- 801 Raimonet, M., & Cloern, J. E. (2017). Estuary–ocean connectivity: Fast physics, slow biology.
802 *Global Change Biology*, 23(6), 2345–2357. <https://doi.org/10.1111/gcb.13546>
- 803 Raymond, P. A., & Cole, J. J. (2001). Gas exchange in rivers and estuaries: Choosing a gas
804 transfer velocity. *Estuaries*, 24(2), 312–317. <https://doi.org/10.2307/1352954>
- 805 Raymond, P. A., Zappa, C. J., Butman, D., Bott, T. L., Potter, J., Mulholland, P., Laursen, A. E.,
806 McDowell, W. H., & Newbold, D. (2012). Scaling the gas transfer velocity and hydraulic
807 geometry in streams and small rivers: Gas transfer velocity and hydraulic geometry.
808 *Limnology and Oceanography: Fluids and Environments*, 2(1), 41–53.
809 <https://doi.org/10.1215/21573689-1597669>
- 810 Redfield, A. C. (1934). On the Properties of Organic Derivatives in Sea Water and Their
811 Relation to Composition of the Phytoplankton. In *James Johnstone Memorial Volume*
812 (pp. 176–192). University Press of Liverpool.
- 813 Reisinger, A. J., Groffman, P. M., & Rosi-Marshall, E. J. (2016). Nitrogen-cycling process rates
814 across urban ecosystems. *FEMS Microbiology Ecology*, 92(12), fiw198.
815 <https://doi.org/10.1093/femsec/fiw198>
- 816 Reisinger, A. J., Rosi, E. J., Bechtold, H. A., Doody, T. R., Kaushal, S. S., & Groffman, P. M.
817 (2017). Recovery and resilience of urban stream metabolism following Superstorm
818 Sandy and other floods. *Ecosphere*, 8(4), e01776. <https://doi.org/10.1002/ecs2.1776>
- 819 Russell, S. J., Windham-Myers, L., Stuart-Haëntjens, E. J., Bergamaschi, B. A., Anderson, F.,
820 Oikawa, P., & Knox, S. H. (2023). Increased salinity decreases annual gross primary
821 productivity at a Northern California brackish tidal marsh. *Environmental Research*
822 *Letters*, 18(3), 034045. <https://doi.org/10.1088/1748-9326/acbbdf>
- 823 Schimel, J. P., & Bennett, J. (2004). Nitrogen Mineralization: Challenges of a Changing
824 Paradigm. *Ecology*, 85(3), 591–602. <https://doi.org/10.1890/03-8002>

- 825 Schindler, D. W. (1977). Evolution of Phosphorus Limitation in Lakes. *Science*, 195(4275), 260–
826 262. <https://doi.org/10.1126/science.195.4275.260>
- 827 Scully, M. E. (2010). Wind Modulation of Dissolved Oxygen in Chesapeake Bay. *Estuaries and*
828 *Coasts*, 33(5), 1164–1175. <https://doi.org/10.1007/s12237-010-9319-9>
- 829 Simon, A., & Rinaldi, M. (2006). Disturbance, stream incision, and channel evolution: The roles
830 of excess transport capacity and boundary materials in controlling channel response.
831 *Geomorphology*, 79(3), 361–383. <https://doi.org/10.1016/j.geomorph.2006.06.037>
- 832 Smith, B. K., & Smith, J. A. (2015). The Flashiest Watersheds in the Contiguous United States.
833 *Journal of Hydrometeorology*, 16(6), 2365–2381. [https://doi.org/10.1175/JHM-D-14-](https://doi.org/10.1175/JHM-D-14-0217.1)
834 0217.1
- 835 Smith, S. V. (1984). Phosphorus versus nitrogen limitation in the marine environment.
836 *Limnology and Oceanography*, 29(6), 1149–1160.
837 <https://doi.org/10.4319/lo.1984.29.6.1149>
- 838 Song, C., Dodds, W. K., Rüegg, J., Argerich, A., Baker, C. L., Bowden, W. B., Douglas, M. M.,
839 Farrell, K. J., Flinn, M. B., Garcia, E. A., Helton, A. M., Harms, T. K., Jia, S., Jones, J. B.,
840 Koenig, L. E., Kominoski, J. S., McDowell, W. H., McMaster, D., Parker, S. P., ...
841 Ballantyne, F. (2018). Continental-scale decrease in net primary productivity in streams
842 due to climate warming. *Nature Geoscience*, 11(6), Article 6.
843 <https://doi.org/10.1038/s41561-018-0125-5>
- 844 Sullivan, B. W., Alvarez-Clare, S., Castle, S. C., Porder, S., Reed, S. C., Schreeg, L.,
845 Townsend, A. R., & Cleveland, C. C. (2014). Assessing nutrient limitation in complex
846 forested ecosystems: Alternatives to large-scale fertilization experiments. *Ecology*,
847 95(3), 668–681. <https://doi.org/10.1890/13-0825.1>
- 848 Toseland, A., Daines, S. J., Clark, J. R., Kirkham, A., Strauss, J., Uhlig, C., Lenton, T. M.,
849 Valentin, K., Pearson, G. A., Moulton, V., & Mock, T. (2013). The impact of temperature
850 on marine phytoplankton resource allocation and metabolism. *Nature Climate Change*,
851 3(11), Article 11. <https://doi.org/10.1038/nclimate1989>
- 852 Uehlinger, U. (2000). Resistance and resilience of ecosystem metabolism in a flood-prone river
853 system. *Freshwater Biology*, 45(3), 319–332. [https://doi.org/10.1111/j.1365-](https://doi.org/10.1111/j.1365-2427.2000.00620.x)
854 2427.2000.00620.x
- 855 Van Meerbeek, K., Jucker, T., & Svenning, J.-C. (2021). Unifying the concepts of stability and
856 resilience in ecology. *Journal of Ecology*, 109(9), 3114–3132.
857 <https://doi.org/10.1111/1365-2745.13651>
- 858 Vietz, G. J., Walsh, C. J., & Fletcher, T. D. (2016). Urban hydrogeomorphology and the urban

- 859 stream syndrome: Treating the symptoms and causes of geomorphic change. *Progress*
860 *in Physical Geography: Earth and Environment*, 40(3), 480–492.
861 <https://doi.org/10.1177/0309133315605048>
- 862 Vitousek, P. M., & Howarth, R. W. (1991). Nitrogen limitation on land and in the sea: How can it
863 occur? *Biogeochemistry*, 13(2), 87–115. <https://doi.org/10.1007/BF00002772>
- 864 Walsh, C. J., Roy, A. H., Feminella, J. W., Cottingham, P. D., Groffman, P. M., & Morgan, R. P.
865 (2005). The urban stream syndrome: Current knowledge and the search for a cure.
866 *Journal of the North American Benthological Society*, 24(3), 706–723.
867 <https://doi.org/10.1899/04-028.1>
- 868 Wang, J., & Zhang, Z. (2020). Phytoplankton, dissolved oxygen and nutrient patterns along a
869 eutrophic river-estuary continuum: Observation and modeling. *Journal of Environmental*
870 *Management*, 261, 110233. <https://doi.org/10.1016/j.jenvman.2020.110233>
- 871 Woodland, R. J., Thomson, J. R., Mac Nally, R., Reich, P., Evrard, V., Wary, F. Y., Walker, J.
872 P., & Cook, P. L. M. (2015). Nitrogen loads explain primary productivity in estuaries at
873 the ecosystem scale. *Limnology and Oceanography*, 60(5), 1751–1762.
874 <https://doi.org/10.1002/lno.10136>
- 875 Zahn, E., Welty, C., Smith, J. A., Kemp, S. J., Baeck, M.-L., & Bou-Zeid, E. (2021). The
876 Hydrological Urban Heat Island: Determinants of Acute and Chronic Heat Stress in
877 Urban Streams. *JAWRA Journal of the American Water Resources Association*, 57(6),
878 941–955. <https://doi.org/10.1111/1752-1688.12963>
- 879 Zhang, J., Gilbert, D., Gooday, A. J., Levin, L., Naqvi, S. W. A., Middelburg, J. J., Scranton, M.,
880 Ekau, W., Peña, A., Dewitte, B., Oguz, T., Monteiro, P. M. S., Urban, E., Rabalais, N. N.,
881 Ittekkot, V., Kemp, W. M., Ulloa, O., Elmgren, R., Escobar-Briones, E., & Van der Plas,
882 A. K. (2010). Natural and human-induced hypoxia and consequences for coastal areas:
883 Synthesis and future development. *Biogeosciences*, 7(5), 1443–1467.
884 <https://doi.org/10.5194/bg-7-1443-2010>
- 885 Zhang, M., Krom, M. D., Lin, J., Cheng, P., & Chen, N. (2022). Effects of a Storm on the
886 Transformation and Export of Phosphorus Through a Subtropical River-Turbid Estuary
887 Continuum Revealed by Continuous Observation. *Journal of Geophysical Research:*
888 *Biogeosciences*, 127(8), e2022JG006786. <https://doi.org/10.1029/2022JG006786>
- 889 Zhang, Q., Fisher, T. R., Trentacoste, E. M., Buchanan, C., Gustafson, A. B., Karrh, R., Murphy,
890 R. R., Keisman, J., Wu, C., Tian, R., Testa, J. M., & Tango, P. J. (2021). Nutrient
891 limitation of phytoplankton in Chesapeake Bay: Development of an empirical approach
892 for water-quality management. *Water Research*, 188, 116407.

893 <https://doi.org/10.1016/j.watres.2020.116407>
894 Zheng, Y., Huang, J., Feng, Y., Xue, H., Xie, X., Tian, H., Yao, Y., Luo, L., Guo, X., & Liu, Y.
895 (2024). The Effects of Seasonal Wind Regimes on the Evolution of Hypoxia in
896 Chesapeake Bay: Results from A Terrestrial-Estuarine-Ocean Biogeochemical Modeling
897 System. *Progress in Oceanography*, 103207.
898 <https://doi.org/10.1016/j.pocean.2024.103207>
899

900 *Data Availability Statement:*

901 This study used publicly available datasets, which included: 1) Long-term estuarine water
902 quality, nutrients and meteorological conditions and watershed boundaries for Lake Superior
903 (LKS) NERR, Chesapeake Bay, Maryland (CBM) NERR, Guana Tolomato Matanzas (GTM)
904 NERR, Weeks Bay (WKB) NERR, and San Francisco Bay (SFB) NERR stations from
905 <https://cdmo.baruch.sc.edu>; 2) Long-term precipitation data from U.S. airports from
906 <https://www.ncei.noaa.gov/cdo-web/datasets>; 3) Land use/land cover maps from
907 <https://livingatlas.arcgis.com/landcover/>; 4) U.S. population data from
908 <https://www.worldpop.org/>.

909

910 *Author Contribution Statement*

911 E.B.G. and A.B.T. developed the study and interpreted the results. A.B.T. performed data
912 analysis and drafted the manuscript. All authors contributed to manuscript editing.

913

914 **Supplementary Material for:**

915

916 **Title.** Physicochemical Factors and Urban Land-Use Characteristics Associated with Resistance
917 to Precipitation in Estuaries Vary Across Scales

918

919 **Authors and Affiliations**

920 *Anna B. Turetcaia 0000-0003-1630-5741¹, anna.turetcaia@pnnl.gov*

921 *Nicole G. Dix 0000-0002-0063-5167², nikki.dix@dep.state.fl.us*

922 *Hannah Ramage 0009-0004-2246-7696³, hannah.ramage@wisc.edu*

923 *Matthew C. Ferner 0000-0002-4862-9663⁴, mferner@sfsu.edu*

924 *and Emily B. Graham 0000-0002-4623-7076^{1,5}, emily.graham@pnnl.gov*

925

926 ¹ Pacific Northwest National Laboratory, Richland, WA 99352, USA

927 ² Guana Tolomato Matanzas National Estuarine Research Reserve, Ponte Vedra Beach, FL
928 32082, USA

929 ³ Lake Superior National Estuarine Research Reserve, University of Wisconsin Madison,
930 Division of Extension, Superior, WI 54880, USA

931 ⁴ San Francisco State University, Estuary and Ocean Science Center, Tiburon, CA 94920, USA

932 ⁵ School of Biological Sciences, Washington State University, Pullman, WA 99164, USA

933

934 **Corresponding authors:** *Anna B. Turetcaia (anna.turetcaia@pnnl.gov) and Emily B. Graham*
935 *(emily.graham@pnnl.gov)*

936

937

938 **Supplementary Tables.**

939
 940 **Table S1.** Threshold value for major precipitation events and breakdown of the number of events
 941 during wet and dry years at each National Estuarine Research Reserve (NERR) station.

NERR Station	Date:Time used to select dissolved oxygen and precipitation measurements to calculate the resistance index		Precip. event (mm)	Wet/Dry year	precip. threshold (mm/day)
	Prior to disturbance (C ₀)	During and post disturbance (P ₀)			
Lake Superior, WI (LKS)	2017/06/24 00:00:00 -2017/06/27 23:45:00	2017/06/28 06:00:00 -2017/06/29 23:45:00	34.4	Wet (4)	> 25
	2017/07/30 00:00:00 -2017/08/02 23:45:00	2017/08/03 00:00:00 -2017/08/04 23:45:00	38.1		
	2017/08/23 00:00:00 -2017/08/25 23:45:00	2017/08/26 00:00:00 -2017/08/28 23:45:00	61.0		
	2017/09/29 00:00:00 -2017/10/01 23:45:00	2017/10/02 00:00:00 -2017/10/05 23:45:00	44.2		
	2020/07/14 00:00:00 -2020/07/17 23:45:00	2020/07/18 00:00:00 -2020/07/19 23:45:00	42.9	Dry (3)	
	2020/07/14 00:00:00 -2020/07/17 23:45:00	2020/07/21 00:00:00 -2020/07/23 23:45:00	29.6		
2020/08/04 00:00:00 -2020/08/06 23:45:00	2020/08/07 12:00:00 -2020/08/11 23:45:00	74.9			
Chesapeake Bay, MD (CBM)	2018/05/10 00:00:00 -2018/05/11 12:00:00	2018/05/16 00:00:00 -2018/05/21 23:45:00	117.1	Wet (7)	>25
	2018/05/24 00:00:00 -2018/05/26 23:45:00	2018/05/27 15:00:00 -2018/05/28 23:45:00	40.2		
	2018/05/24 00:00:00 -2018/05/26 23:45:00	2018/06/03 06:00:00 -2018/06/07 23:45:00	56.2		
	2018/06/16 00:00:00 -2018/06/18 23:45:00	2018/06/19 12:00:00 -2018/06/25 23:45:00	41.8		
	2018/07/13 00:00:00 -2018/07/16 23:45:00	2018/07/21 12:00:00 -2018/07/27 23:45:00	218.1		
	2018/09/04 00:00:00 -2018/09/06 23:45:00	2018/09/09 00:00:00 -2018/09/10 23:45:00	49.1		
	2018/09/13 00:00:00 -2018/09/15 23:45:00	2018/09/23 00:00:00 -2018/09/25 23:45:00	58.6		
	2016/06/24 00:00:00 -2016/06/27 23:45:00	2016/07/01 12:00:00 -2016/07/02 23:45:00	41.0	Dry (3)	
	2016/09/15 00:00:00 -2016/09/18 23:45:00	2016/09/19 00:00:00 -2016/09/19 23:45:00	25.2		
	2016/09/23 00:00:00 -2016/09/25 23:45:00	2016/09/28 00:00:00 -2016/09/30 23:45:00	76.4		
Guana Tolomato Matanzas, FL (GTM)	2017/08/19 00:00:00 -2017/08/22 23:45:00	2017/09/10 00:00:00 -2017/09/21 23:45:00	222.9	Wet (3)	*
	2017/08/19 00:00:00 -2017/08/22 23:45:00	2017/09/30 00:00:00 -2017/10/13 23:45:00	270.7		
	2017/11/15 00:00:00 -2017/11/22 23:45:00	2017/11/23 00:00:00 -2017/11/25 23:45:00	123.1		
	2016/06/01 00:00:00 -2016/06/04 23:45:00	2016/06/05 12:00:00 -2016/06/07 23:45:00	127.9	Dry (4)	
	2016/08/21 00:00:00 -2016/08/27 23:45:00	2016/08/28 00:00:00 -2016/09/06 23:45:00	67.2		
	2016/09/05 00:00:00 -2016/09/08 23:45:00	2016/09/14 00:00:00 -2016/09/19 23:45:00	27.3		
	2016/09/21 00:00:00 -2016/09/25 23:45:00	2016/09/28 00:00:00 -2016/10/17 23:45:00	193.3		
Weeks Bay, AL (WKB)	2018/05/19 00:00:00 -2018/05/22 23:45:00	2018/05/23 00:00:00 -2018/05/27 23:45:00	90.9	Wet (8)	> 30
	2018/06/07 00:00:00 -2018/06/09 23:45:00	2018/06/11 00:00:00 -2018/06/13 23:45:00	47.0		
	2018/06/28 00:00:00 -2018/06/30 23:45:00	2018/07/01 12:00:00 -2018/07/09 23:45:00	86.3		
	2018/07/12 00:00:00 -2018/07/14 23:45:00	2018/07/16 09:00:00 -2018/07/18 23:45:00	53.7		

	2018/08/25 00:00:00 -2018/08/26 23:45:00 2018/08/25 00:00:00 -2018/08/26 23:45:00 2018/09/19 00:00:00 -2018/09/20 23:45:00 2018/09/19 00:00:00 -2018/09/20 23:45:00	2018/09/01 00:00:00 -2018/09/03 23:45:00 2018/09/04 00:00:00 -2018/09/08 23:45:00 2018/09/21 12:00:00 -2018/09/23 23:45:00 2018/09/24 00:00:00 -2018/09/29 23:45:00	56.6 128.6 46.7 66.5		
	2019/04/01 00:00:00 -2019/04/03 23:45:00 2019/04/15 00:00:00 -2019/04/17 23:45:00 2019/06/01 00:00:00 -2019/06/04 23:45:00 2019/06/20 00:00:00 -2019/06/25 23:45:00 2019/08/07 00:00:00 -2019/08/10 23:45:00 2019/08/22 00:00:00 -2019/08/24 23:45:00 2019/10/21 00:00:00 -2019/10/24 23:45:00	2019/04/04 09:00:00 -2019/04/04 23:45:00 **2019/04/26 15:00:00 -2019/04/28 23:45:00 2019/06/06 00:00:00 -2019/06/13 23:45:00 2019/07/13 00:00:00 -2019/07/15 23:45:00 2019/08/15 12:00:00 -2019/08/16 23:45:00 2019/08/26 06:00:00 -2019/08/27 06:00:00 2019/10/30 00:00:00 -2019/11/01 23:45:00	40.0 32.9 116.1 89.1 37.0 48.2 61.8	Dry (7)	
San Francisco Bay, CA (SFB)	2017/01/01 00:00:00 -2017/01/02 06:00:00 2017/01/01 00:00:00 -2017/01/02 06:00:00 2017/01/01 00:00:00 -2017/01/02 06:00:00 2017/03/11 00:00:00 -2017/03/17 23:45:00 2017/04/01 00:00:00 -2017/04/05 06:00:00	2017/01/03 00:00:00 -2017/01/06 00:00:00 2017/01/07 00:00:00 -2017/01/12 23:45:00 2017/01/18 00:00:00 -2017/01/25 00:00:00 2017/03/20 00:00:00 -2017/03/23 23:45:00 2017/04/06 20:00:00 -2017/04/07 23:45:00	38.7 126.4 110.8 43.0 37.0	Wet (5)	> 20
	2018/01/06 00:00:00 -2018/01/07 23:45:00 2018/02/20 00:00:00 -2018/02/23 23:45:00 2018/04/04 12:00:00 -2018/04/05 12:00:00	2018/01/08 00:00:00 -2018/01/09 23:45:00 ***2018/03/01 00:00:00 -2018/03/01 23:45:00 2018/04/06 00:00:00 -2018/04/07 23:45:00	73.6 30.7 54.6	Dry (3)	
<p>* For GTM 2016 the selected events were: Colin, Julia, Hermine, and Matthew. For 2017 the events were Irma and two Nor'easters.</p> <p>** This resistance calculation does not include dissolved oxygen measurements during the actual rain event from 2019/04/25 only dissolved oxygen after the event, because data during the event is missing from MB monitoring location.</p> <p>*** Dissolved oxygen data for the SM site is missing. No resistance was calculated for SM during that time.</p>					

942

943

944 **Supplementary figures.**

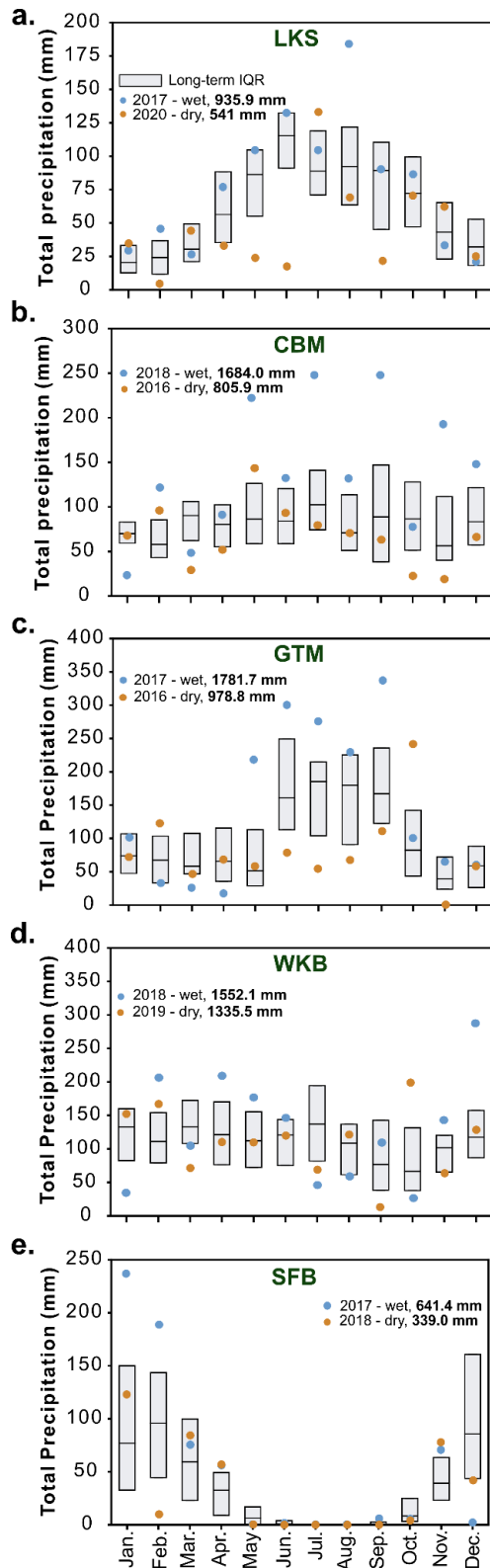
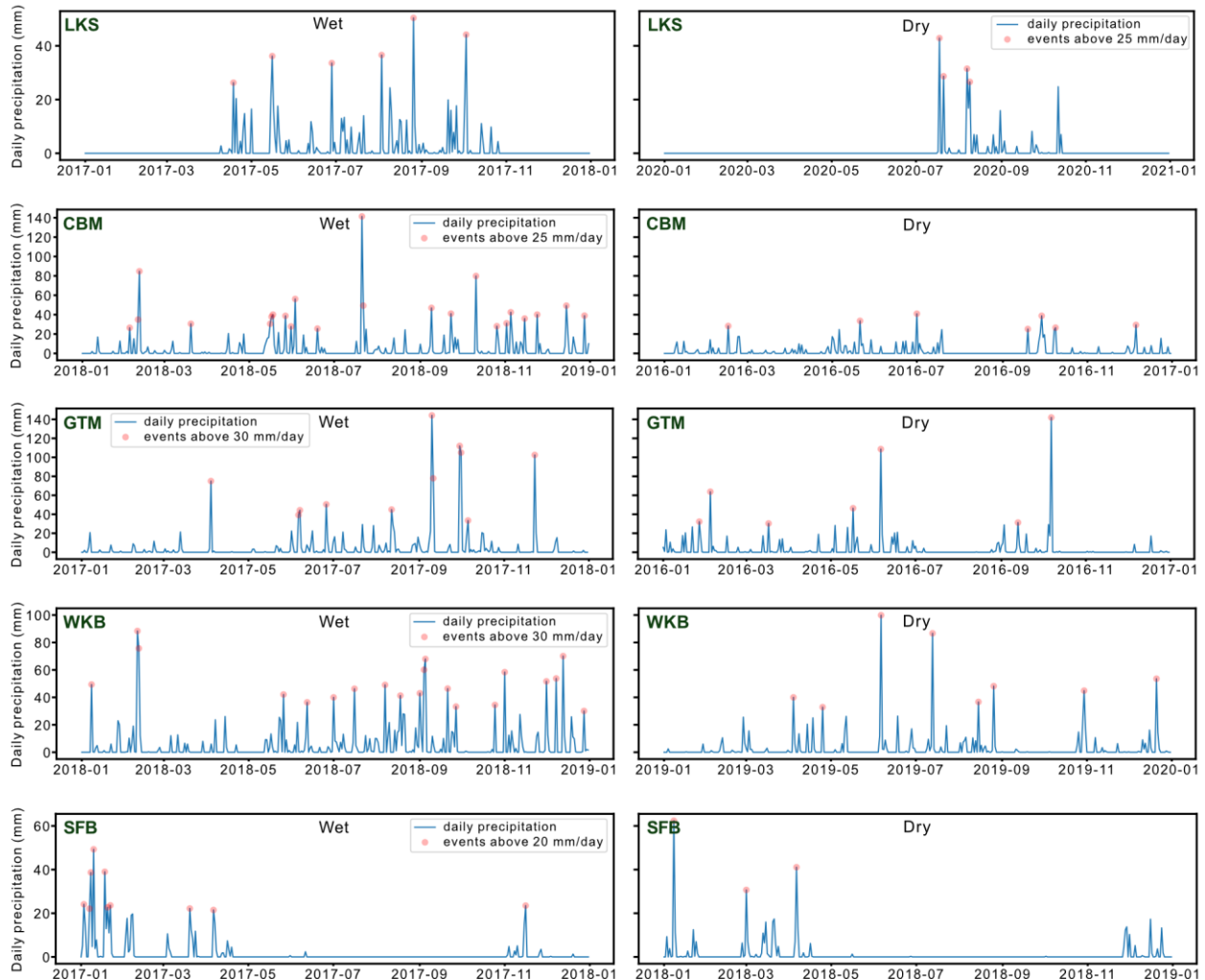


Fig. S1. Long-term (30-year) interquartile range and monthly precipitation during relatively wet and dry years. Long term precipitation data obtained from airports located in the vicinity of each selected estuarine station. a) Precipitation records from Duluth International airport were used to infer wet/dry years at Lake Superior (LKS) station. b) Washington Reagan International Airport precipitation records were used for Chesapeake Bay (CBM) station. c) Jacksonville International Airport precipitation record was used for Guana Tolomato Matanzas (GTM) station. d) Birmingham Airport precipitation records were used for Weeks Bay (WKS) station. e) San Francisco International Airport precipitation records were used for San Francisco Bay (SFB) station.



946

947

948

949

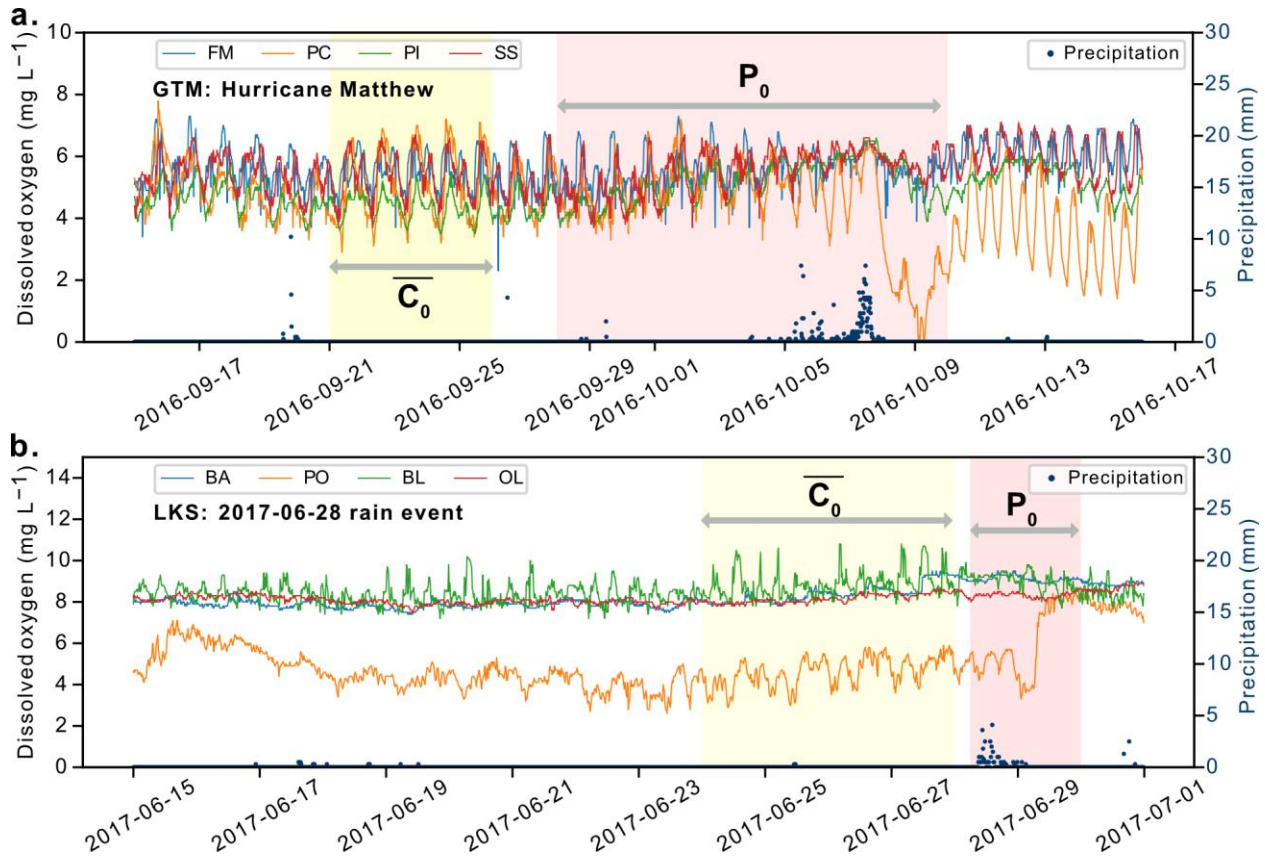
950

951

952

953

Fig. S2. Major precipitation events for each estuary during wet and dry years. The major precipitation events (red circles) were identified by plotting National Estuarine Research Reserve (NERR) precipitation data collected at each estuary. The events were down-selected based on water quality data availability for each estuary. Estuary abbreviations: Lake Superior (LKS) NERR, Chesapeake Bay, Maryland (CBM) NERR, Guana Tolomato Matanzas (GTM) NERR, Weeks Bay (WKB) NERR, and San Francisco Bay (SFB) NERR. For details about events used for resistance index calculations, please see Table S1.



954

955 **Fig. S3.** Example for visualizing the selection of variables for resistance index calculations.

956 Yellow shaded box indicates the time used to calculate average pre-disturbance dissolved oxygen

957 concentration (average C_0). Red shaded box indicated the time used to identify dissolved oxygen

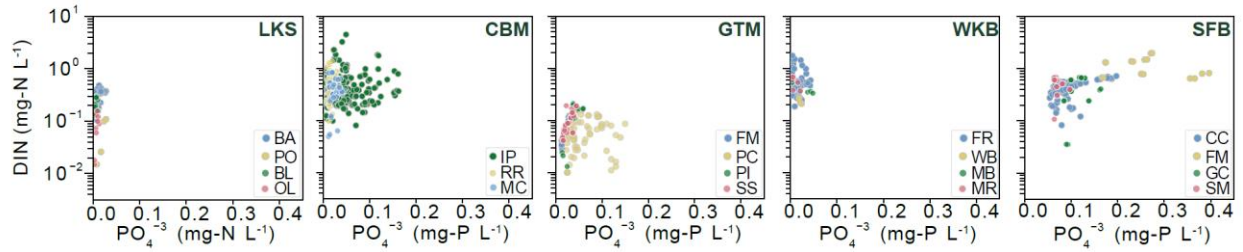
958 concentration post-disturbance (P_0). P_0 was identified as the maximum displacement from

959 average C_0 . a) Dissolved oxygen and precipitation at Guana Tolomato Matanzas (GTM) National

960 Estuarine Research Reserve (NERR) during hurricane Matthew. b) Dissolved oxygen and

961 precipitation at Lake Superior (LKS) NERR during a precipitation event on 06-28-2017.

962



963

964

965

966

967

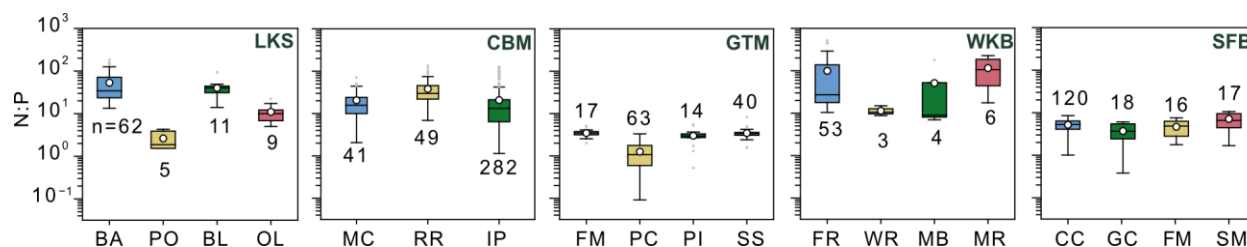
968

969

970

Fig. S4. Dissolved inorganic nutrient concentrations at each estuary. Dissolved inorganic nitrogen (DIN) (i.e., $\text{NO}_3^- + \text{NO}_2^- + \text{NH}_4^+$). Estuary abbreviations: Lake Superior (LKS) NERR, Chesapeake Bay, Maryland (CBM) NERR, Guana Tolomato Matanzas (GTM) NERR, Weeks Bay (WKB) NERR, and San Francisco Bay (SFB) NERR. For LKS estuary, the NH_4^+ measurements for dry-year (2020) were missing at all monitoring locations. For WKB, the PO_4^{3-} measurements for wet-year (2018) were missing at WB, MB, and MR monitoring locations.

971



972

973

974

975

976

977

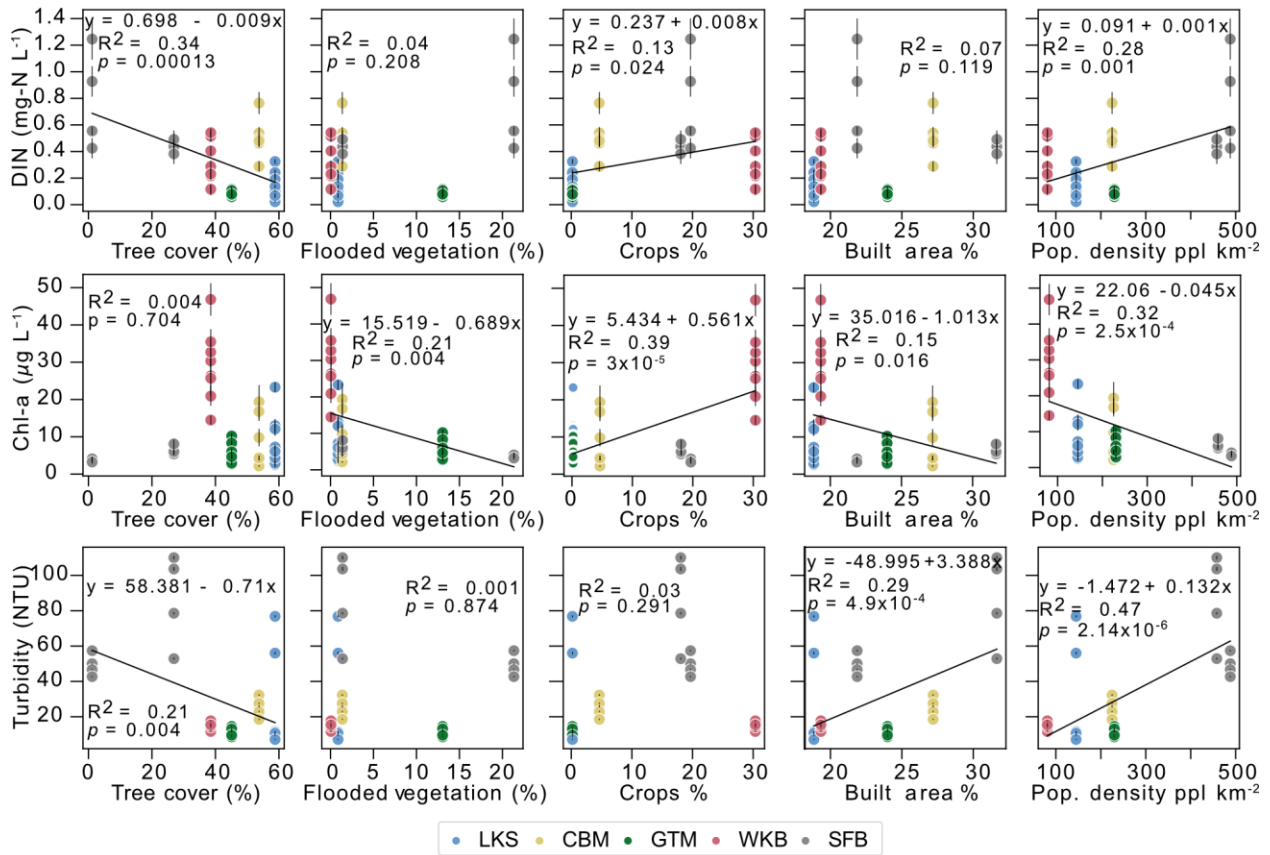
978

979

980

Fig. S5. Variation in resistance within individual estuaries. Estuary abbreviations: Lake Superior (LKS) NERR, Chesapeake Bay, Maryland (CBM) NERR, Guana Tolomato Matanzas (GTM) NERR, Weeks Bay (WKB) NERR, and San Francisco Bay (SFB) NERR. Means are shown in white circles, and medians are shown in black solid lines. Boxes show the quartiles of the dataset and the whiskers show the rest of the distribution. The stoichiometric N:P ratio was calculated using dissolved inorganic nitrogen species (i.e., $\text{NO}_3^- + \text{NO}_2^- + \text{NH}_4^+$) and phosphate. We note that because of missing measurements for PO_4^{3-} during the wet year at WKB- WB, MB, and MR – the N:P ratios at these locations were calculated only for the dry year.

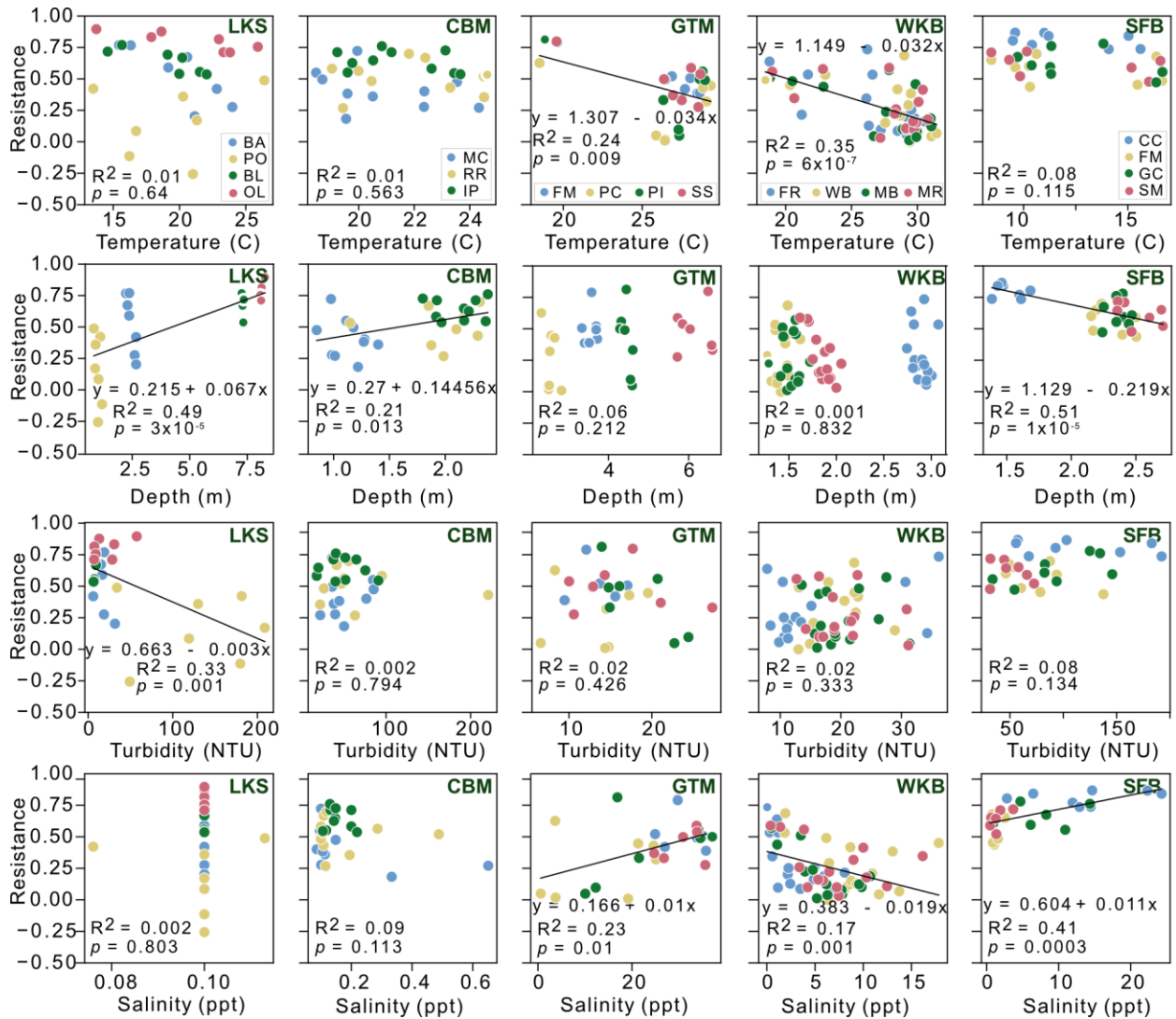
981



982

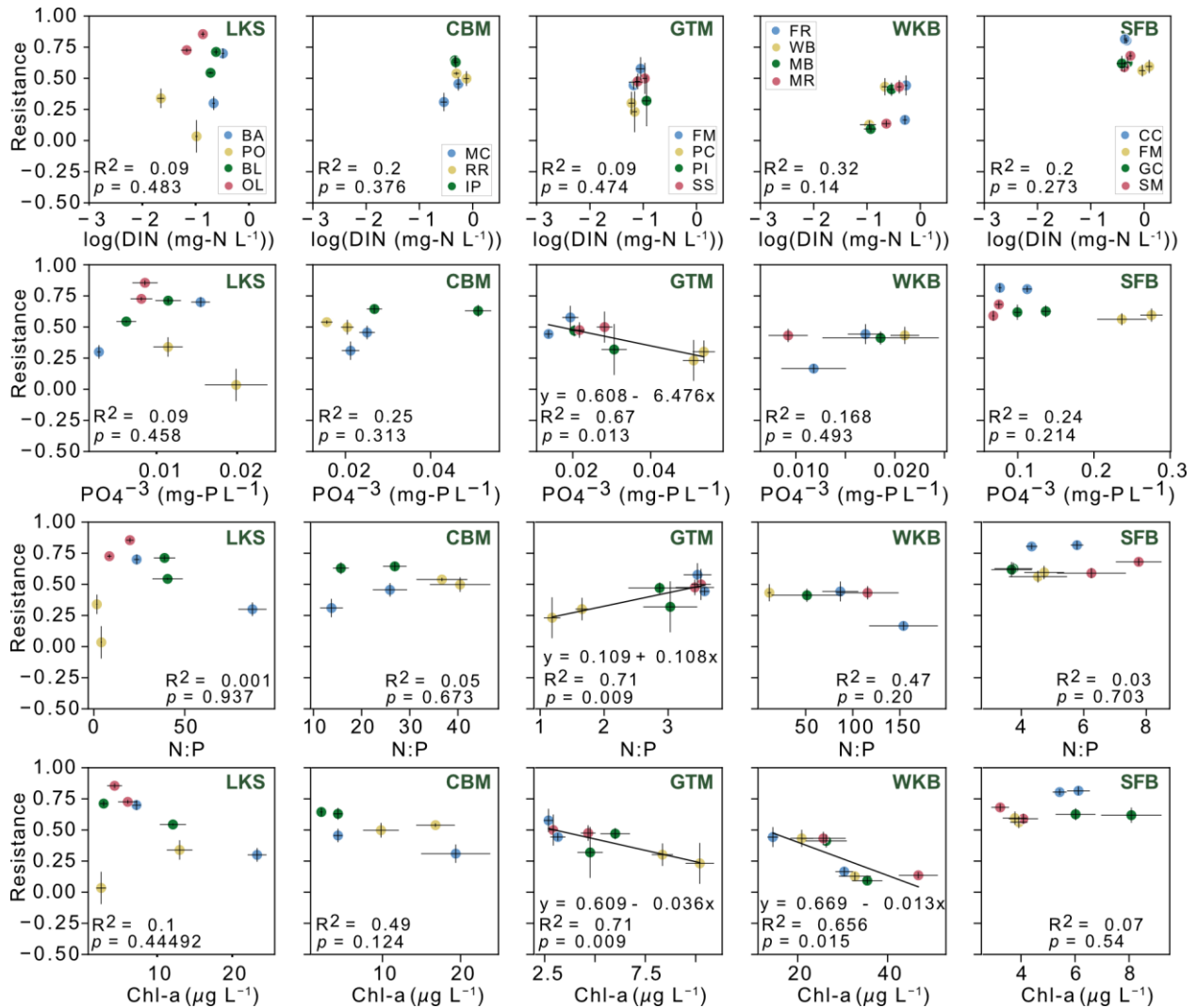
983 **Fig. S6.** Relationships of dissolved inorganic nitrogen (DIN), chlorophyll-*a* (Chl-*a*), and
 984 turbidity to land use/land cover and population density. Estuary abbreviations: Lake Superior
 985 (LKS) NERR, Chesapeake Bay, Maryland (CBM) NERR, Guana Tolomato Matanzas (GTM)
 986 NERR, Weeks Bay (WKB) NERR, and San Francisco Bay (SFB) NERR. Regressions for
 987 significant relationships (p-value < 0.05) are shown in black lines. All relationships use annual
 988 means for physicochemical factors calculated for wet and dry years separately and land use/land
 989 cover characteristics adjoined to monitoring locations at each estuary.

990



991
 992 **Fig. S7.** Relationships of resistance to water temperature, water column depth, turbidity, and
 993 salinity at each estuary. Estuary abbreviations: Lake Superior (LKS) NERR, Chesapeake Bay,
 994 Maryland (CBM) NERR, Guana Tolomato Matanzas (GTM) NERR, Weeks Bay (WKB) NERR,
 995 and San Francisco Bay (SFB) NERR. Significant correlations ($p < 0.05$) are shown in black
 996 lines. Relationships consider mean values of physicochemical factors in context of precipitation
 997 events used in resistance index calculations (see dates for P_0 in Table S1).

998
 999



1000
 1001 **Fig. S8.** Relationships of resistance to dissolved inorganic nitrogen (DIN), phosphate (PO₄³⁻),
 1002 N:P ratio, and chlorophyll-*a* (Chl-*a*) at each estuary. Estuary abbreviations: Lake Superior (LKS)
 1003 NERR, Chesapeake Bay, Maryland (CBM) NERR, Guana Tolomato Matanzas (GTM) NERR,
 1004 Weeks Bay (WKB) NERR, and San Francisco Bay (SFB) NERR. Significant correlations ($p <$
 1005 0.05) are shown in black. Standard errors of the mean are shown in horizontal and vertical black
 1006 lines. Relationships consider annual mean values of resistance and annual mean values for
 1007 nutrients, N:P, and Chl-*a* calculated for wet and dry years separately.